

---

# Chapter 5

## BEAMS AND FRAMES

---

### 5.1 INTRODUCTION

Here we consider the finite element formulation of the one-dimensional fourth-order differential equation that arises in the Euler–Bernoulli beam theory and the pair of one-dimensional second-order equations associated with the Timoshenko beam theory. The superposition of the beam and bar elements give rise to frame elements that can be used to analyze plane frame structures. The formulations of a fourth-order equation as well as coupled second-order equations (see Problems 3.1 and 3.3) involve the same steps as described in Section 3.2 for a second-order equation, but the mathematical details are somewhat different, especially in the finite element formulation of the equations.

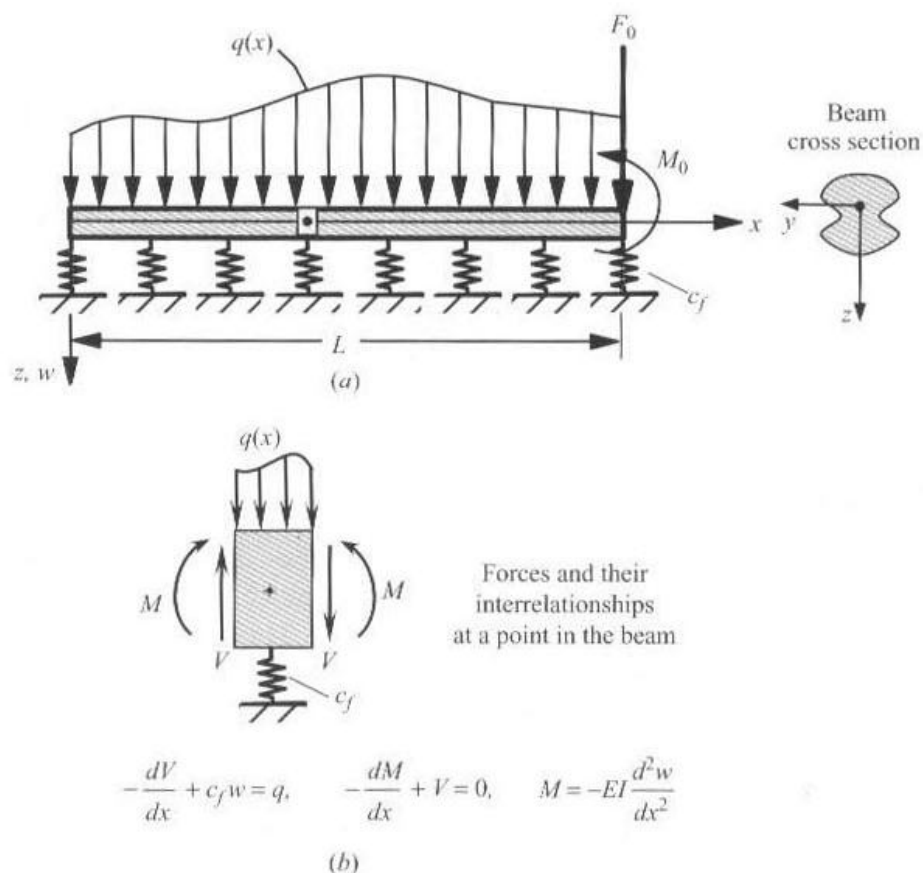
### 5.2 EULER–BERNOULLI BEAM ELEMENT

#### 5.2.1 Governing Equation

In the Euler–Bernoulli beam theory, it is assumed that plane cross sections perpendicular to the axis of the beam remain plane and perpendicular to the axis after deformation. In this theory, the transverse deflection  $w$  of the beam is governed by the fourth-order differential equation

$$\frac{d^2}{dx^2} \left( EI \frac{d^2 w}{dx^2} \right) + c_f w = q(x) \quad \text{for } 0 < x < L \quad (5.2.1)$$

where  $EI = E(x)I(x)$ ,  $c_f = c_f(x)$ ,  $q = q(x)$  are given functions of  $x$  (i.e., data), and  $w$  is the dependent variable;  $E$  denotes the modulus of elasticity,  $I$  the second moment of area about the  $y$  axis of the beam,  $q$  is the distributed transverse load,  $c_f$  the elastic foundation modulus (if any), and  $w$  is the transverse deflection of the beam. The sign convention used in the derivation of (5.2.1) is shown in Fig. 5.2.1. In addition to satisfying the differential equation (5.2.1),  $w$  must also satisfy appropriate boundary conditions; since the equation is of fourth order, four boundary conditions are needed to solve it. The weak formulation of the equation will provide the form of these four boundary conditions. A step-by-step procedure for the finite element analysis of (5.2.1) is presented next (see Example 2.4.2).



**Figure 5.2.1** (a) Typical beam with distributed load  $q(x)$  and point force  $F_0$  and moment  $M_0$ . (b) The shear force-bending moment-deflection relations and the sign convention.

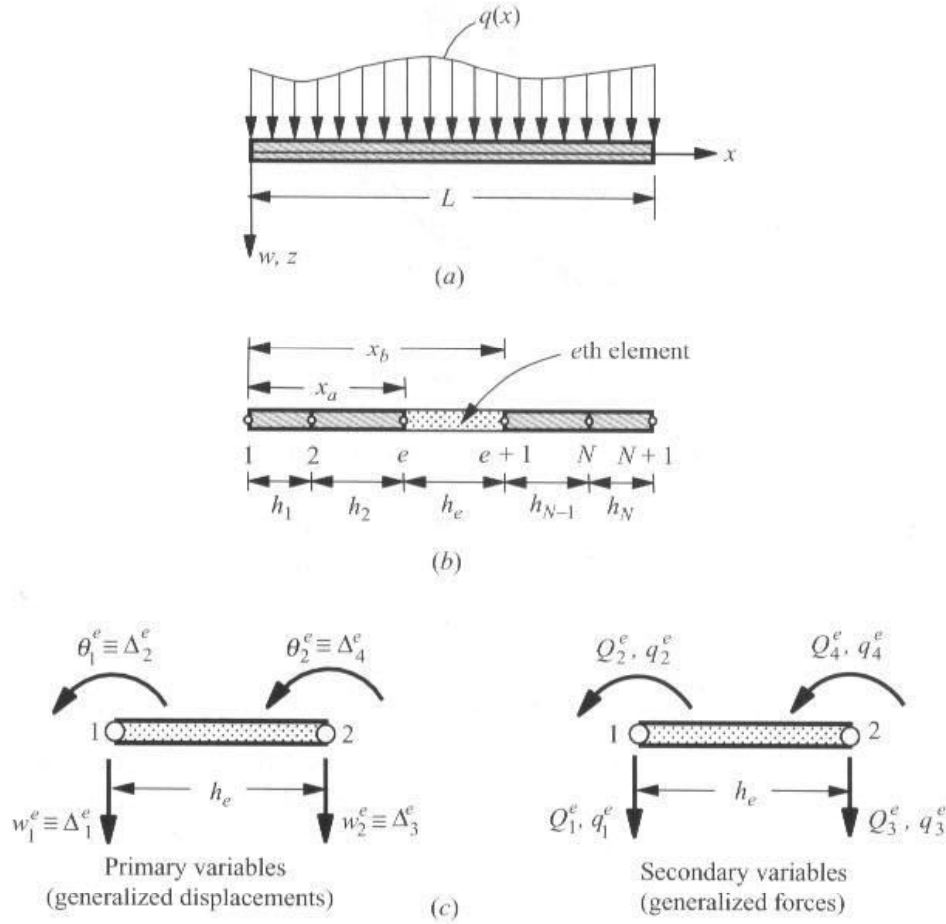
### 5.2.2 Discretization of the Domain

The domain  $\Omega_e = (x_a, x_b) = (x_e, x_{e+1})$  of the straight beam [see Fig. 5.2.2(a)] is divided into a set of  $N$  line elements, each element having at least the two end nodes [see Fig. 5.2.2(b)]. Although the element is geometrically the same as that used for bars, the number and form of the primary and secondary unknowns at each node are dictated by the variational formulation of the differential equation (5.2.1). In most practical problems, the discretization of a given structure into a minimum number of elements is often dictated by the geometry, loading, and material properties.

### 5.2.3 Derivation of Element Equations

We isolate a typical element  $\Omega_e = (x_e, x_{e+1})$  [see Fig. 5.2.2(b)] and construct the weak form of (5.2.1) over the element. The variational formulation provides the primary and secondary variables of the problem. Then suitable approximations for the primary variables are selected, interpolation functions are developed, and the element equations are derived.

**Weak Form.** The weak forms of problems in solid mechanics can be developed either from the principle of virtual work (i.e., the principle of virtual displacements or virtual forces) or from the governing differential equations. Here we start with a given differential equation and use the three-step procedure to obtain the weak form. Following the three-step procedure



**Figure 5.2.2** (a) Geometry and loads on a beam. (b) Finite element discretization. (c) Generalized displacements and generalized forces on a typical element.

illustrated in Chapter 2 (see Example 2.4.2) and revisited in Section 3.2.3, we write

$$\begin{aligned}
 0 &= \int_{x_e}^{x_{e+1}} v \left[ \frac{d^2}{dx^2} \left( EI \frac{d^2 w}{dx^2} \right) + c_f w - q \right] dx \\
 &= \int_{x_e}^{x_{e+1}} \left[ -\frac{dv}{dx} \frac{d}{dx} \left( EI \frac{d^2 w}{dx^2} \right) + c_f v w - v q \right] dx + \left[ v \frac{d}{dx} \left( EI \frac{d^2 w}{dx^2} \right) \right]_{x_e}^{x_{e+1}} \\
 &= \int_{x_e}^{x_{e+1}} \left( EI \frac{d^2 v}{dx^2} \frac{d^2 w}{dx^2} + c_f v w - v q \right) dx + \left[ v \frac{d}{dx} \left( EI \frac{d^2 w}{dx^2} \right) - \frac{dv}{dx} EI \frac{d^2 w}{dx^2} \right]_{x_e}^{x_{e+1}}
 \end{aligned} \tag{5.2.2}$$

where  $v(x)$  is a weight function that is twice differentiable with respect to  $x$ . Note that, in the present case, the first term of the equation is integrated twice by parts, to yield two differentiations to the weight function  $v$  while retaining two derivatives of the dependent variable,  $w$ ; the result is that the differentiation is distributed equally between the weight function  $v$  and the dependent variable  $w$ . Because of the two integration by parts, there appear two boundary expressions (see Example 2.4.2), which are to be evaluated at the two boundary points

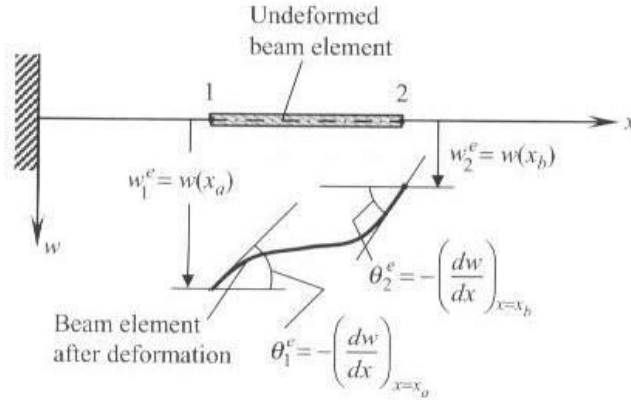


Figure 5.2.3 Deformation of a beam element.

$x = x_a = x_e$  and  $x = x_b = x_{e+1}$ . Examination of the boundary terms indicates that the essential boundary conditions involve the specification of the deflection  $w$  and slope  $dw/dx$ , and the natural boundary conditions involve the specification of the bending moment  $EI d^2w/dx^2$  and shear force  $(d/dx)(EI d^2w/dx^2)$  at the endpoints of the element. Thus, there are two essential boundary conditions and two natural boundary conditions; therefore, we must identify  $w$  and  $dw/dx$  as the primary variables at each node (so that the essential boundary conditions are included in the interpolation). The natural boundary conditions always remain in the weak form and end up on the right-hand side,  $\{F^e\}$ , of the matrix equation.

We introduce the following notation for the secondary variables that is consistent with the sign convention in Fig. 5.2.1(b) ( $\theta = -dw/dx$ ; see Fig. 5.2.3):

$$\begin{aligned} Q_1^e &\equiv \left[ \frac{d}{dx} \left( EI \frac{d^2w}{dx^2} \right) \right] \bigg|_{x_e} = -V(x_e) \\ Q_2^e &\equiv \left( EI \frac{d^2w}{dx^2} \right) \bigg|_{x_e} = -M(x_e) \\ Q_3^e &\equiv - \left[ \frac{d}{dx} \left( EI \frac{d^2w}{dx^2} \right) \right] \bigg|_{x_{e+1}} = V(x_{e+1}) \\ Q_4^e &\equiv - \left( EI \frac{d^2w}{dx^2} \right) \bigg|_{x_{e+1}} = M(x_{e+1}) \end{aligned} \quad (5.2.3)$$

where  $Q_1^e$  and  $Q_3^e$  denote the shear forces, and  $Q_2^e$  and  $Q_4^e$  denote the bending moments [see Fig. 5.2.2c]. The set  $\{Q_1^e, Q_2^e, Q_3^e, Q_4^e\}$  is often referred to as the *generalized forces*. The corresponding displacements and rotations are called the *generalized displacements*.

With the notation in (5.2.3), the weak form (5.2.2) can be expressed as

$$\begin{aligned} 0 &= \int_{x_e}^{x_{e+1}} \left( EI \frac{d^2v}{dx^2} \frac{d^2w}{dx^2} + c_f vw - vq \right) dx \\ &\quad - v(x_e) Q_1^e - \left( -\frac{dv}{dx} \right) \bigg|_{x_e} Q_2^e - v(x_{e+1}) Q_3^e - \left( -\frac{dv}{dx} \right) \bigg|_{x_{e+1}} Q_4^e \\ &\equiv B(v, w) - l(v) \end{aligned} \quad (5.2.4)$$

We can identify the bilinear and linear forms of the problem as

$$\begin{aligned}
 B(v, w) &= \int_{x_e}^{x_{e+1}} \left( EI \frac{d^2 v}{dx^2} \frac{d^2 w}{dx^2} + c_f v w \right) dx \\
 l(v) &= \int_{x_e}^{x_{e+1}} v q \, dx + v(x_e) Q_1^e + \left( -\frac{dv}{dx} \right) \Big|_{x_e} Q_2^e \\
 &\quad + v(x_{e+1}) Q_3^e + \left( -\frac{dv}{dx} \right) \Big|_{x_{e+1}} Q_4^e
 \end{aligned} \tag{5.2.5}$$

Equation (5.2.4) is a statement of the principle of virtual displacements (where  $v$  denotes virtual displacement  $\delta w$ ) for the Euler–Bernoulli beam theory. The quadratic functional, known as the *total potential energy* of the isolated beam element, is given by [see Eq. (2.4.31)]

$$\begin{aligned}
 \Pi_e(w) &= \int_{x_e}^{x_{e+1}} \left[ \frac{EI}{2} \left( \frac{d^2 w}{dx^2} \right)^2 + \frac{1}{2} c_f w^2 - w q \right] dx - w(x_e) Q_1^e - w(x_{e+1}) Q_3^e \\
 &\quad - \left( -\frac{dw}{dx} \right) \Big|_{x_e} Q_2^e - \left( -\frac{dw}{dx} \right) \Big|_{x_{e+1}} Q_4^e
 \end{aligned} \tag{5.2.6}$$

The first term in the square brackets represents the elastic strain energy due to bending, the second is the strain energy stored in the elastic foundation, and the third is the work done by the distributed load; the remaining terms account for the work done by the generalized forces  $Q_i^e$  in moving through the respective generalized displacements of the element. Conversely, we may go from the total potential energy functional (5.2.6) to the weak form (5.2.4) by using the principle of minimum potential energy,  $\delta \Pi^e = 0$ .

**Interpolation Functions.** The variational form (5.2.4) requires that the interpolation functions of an element be continuous with nonzero derivatives up to order two. The approximation  $w_h^e(x)$  of  $w(x)$  over a finite element should be such that it is twice differentiable and satisfies the interpolation properties, i.e., satisfies the following essential “boundary conditions” of the element [see Fig. 5.2.2(c)]:

$$w_h^e(x_e) = w_1^e, \quad w_h^e(x_{e+1}) = w_2^e, \quad \theta_h^e(x_e) = \theta_1^e, \quad \theta_h^e(x_{e+1}) = \theta_2^e \tag{5.2.7}$$

In satisfying the essential boundary conditions (5.2.7), the approximation automatically satisfies the continuity conditions. Hence, we pay attention to the satisfaction of (5.2.7), which forms the basis for the derivation of the interpolation functions of the Euler–Bernoulli beam element.

Since there are a total of four conditions in an element (two per node), a four-parameter polynomial must be selected for  $w_h^e$ :

$$w(x) \approx w_h^e(x) = c_1^e + c_2^e x + c_3^e x^2 + c_4^e x^3 \tag{5.2.8}$$

Note that the continuity conditions (i.e., the existence of a nonzero second derivative of  $w_h^e$  in the element) are automatically met. The next step involves expressing  $c_i^e$  in terms of the primary nodal variables (i.e., generalized displacements)

$$\Delta_1^e \equiv w_h^e(x_e), \quad \Delta_2^e \equiv -\frac{dw_h^e}{dx} \Big|_{x=x_e}, \quad \Delta_3^e \equiv w_h^e(x_{e+1}), \quad \Delta_4^e \equiv -\frac{dw_h^e}{dx} \Big|_{x=x_{e+1}}$$

such that the conditions (5.2.7) are satisfied:

$$\begin{aligned}\Delta_1^e &= w_h^e(x_e) &&= c_1^e + c_2^e x_e + c_3^e x_e^2 + c_4^e x_e^3 \\ \Delta_2^e &= -\frac{dw_h^e}{dx} \Big|_{x=x_e} &&= -c_2^e - 2c_3^e x_e - 3c_4^e x_e \\ \Delta_3^e &= w_h^e(x_{e+1}) &&= c_1^e + c_2^e x_{e+1} + c_3^e x_{e+1}^2 + c_4^e x_{e+1}^3 \\ \Delta_4^e &= -\frac{dw_h^e}{dx} \Big|_{x=x_{e+1}} &&= -c_2^e - 2c_3^e x_{e+1} - 3c_4^e x_{e+1}\end{aligned}$$

or

$$\begin{Bmatrix} \Delta_1^e \\ \Delta_2^e \\ \Delta_3^e \\ \Delta_4^e \end{Bmatrix} = \begin{bmatrix} 1 & x_e & x_e^2 & x_e^3 \\ 0 & -1 & -2x_e & -3x_e^2 \\ 1 & x_{e+1} & x_{e+1}^2 & x_{e+1}^3 \\ 0 & -1 & -2x_{e+1} & -3x_{e+1}^2 \end{bmatrix} \begin{Bmatrix} c_1^e \\ c_2^e \\ c_3^e \\ c_4^e \end{Bmatrix} \quad (5.2.9)$$

Inverting this matrix equation to express  $c_i^e$  in terms of  $\Delta_1^e$ ,  $\Delta_2^e$ ,  $\Delta_3^e$ , and  $\Delta_4^e$ , and substituting the result into (5.2.8), we obtain

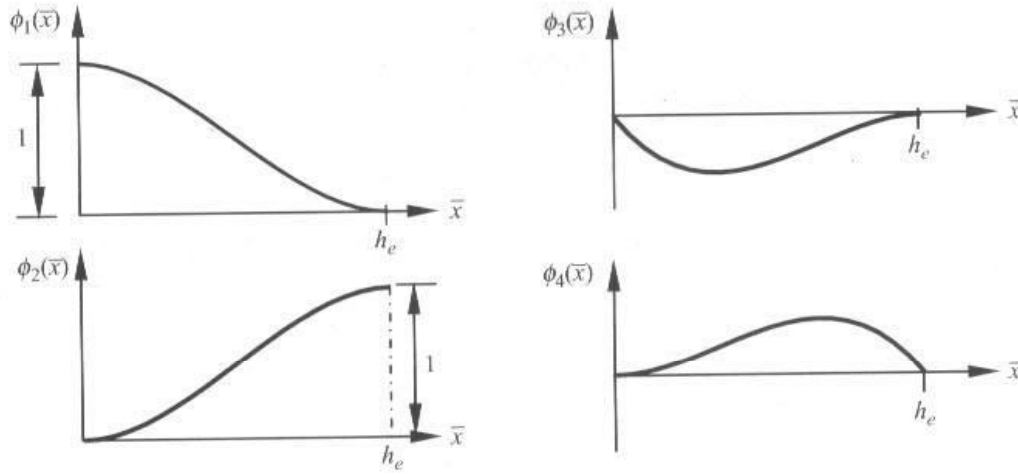
$$w_h^e(x) = \Delta_1^e \phi_1^e + \Delta_2^e \phi_2^e + \Delta_3^e \phi_3^e + \Delta_4^e \phi_4^e = \sum_{j=1}^4 \Delta_j^e \phi_j^e \quad (5.2.10)$$

where (with  $x_{e+1} = x_e + h_e$ )

$$\begin{aligned}\phi_1^e &= 1 - 3 \left( \frac{x - x_e}{h_e} \right)^2 + 2 \left( \frac{x - x_e}{h_e} \right)^3 \\ \phi_2^e &= -(x - x_e) \left( 1 - \frac{x - x_e}{h_e} \right)^2 \\ \phi_3^e &= 3 \left( \frac{x - x_e}{h_e} \right)^2 - 2 \left( \frac{x - x_e}{h_e} \right)^3 \\ \phi_4^e &= -(x - x_e) \left[ \left( \frac{x - x_e}{h_e} \right)^2 - \frac{x - x_e}{h_e} \right]\end{aligned} \quad (5.2.11)$$

Note that the cubic interpolation functions in (5.2.11) are derived by interpolating  $w$  as well as its derivative  $dw/dx$  at the nodes. Such polynomials are known as the *Hermite family of interpolation functions*, and  $\phi_i^e$  in (5.2.11) are called the *Hermite cubic interpolation* (or *cubic spline*) functions. Plots of the Hermite cubic interpolation functions are shown in Fig. 5.2.4.

Recall that the Lagrange cubic interpolation functions are derived to interpolate a function, but not its derivatives, at the nodes. Hence, a Lagrange cubic element will have four nodes, with the dependent variable, not its derivative, as the nodal degree of freedom. Since the slope (or derivative) of the dependent variable is also required by the weak form to be continuous at the nodes for the Euler–Bernoulli beam theory, the Lagrange cubic



**Figure 5.2.4** Hermite cubic interpolations functions used in the Euler-Bernoulli beam element.

interpolation of  $w$ , although it meets the continuity requirement for  $w$ , is *not admissible* in the finite element approximation of the Euler-Bernoulli beam theory.

The interpolation functions  $\phi_i^e$  can be expressed in terms of the local coordinate  $\bar{x} = x - x_e$ :

$$\begin{aligned}\phi_1^e &= 1 - 3\left(\frac{\bar{x}}{h_e}\right)^2 + 2\left(\frac{\bar{x}}{h_e}\right)^3, \quad \phi_2^e = -\bar{x}\left(1 - \frac{\bar{x}}{h_e}\right)^2 \\ \phi_3^e &= 3\left(\frac{\bar{x}}{h_e}\right)^2 - 2\left(\frac{\bar{x}}{h_e}\right)^3, \quad \phi_4^e = -\bar{x}\left[\left(\frac{\bar{x}}{h_e}\right)^2 - \frac{\bar{x}}{h_e}\right]\end{aligned}\quad (5.2.12)$$

The first, second, and third derivatives of  $\phi_i^e$  with respect to  $\bar{x}$  are

$$\frac{d\phi_1^e}{d\bar{x}} = -\frac{6}{h_e}\frac{\bar{x}}{h_e}\left(1 - \frac{\bar{x}}{h_e}\right), \quad \frac{d\phi_2^e}{d\bar{x}} = -\left[1 + 3\left(\frac{\bar{x}}{h_e}\right)^2 - 4\frac{\bar{x}}{h_e}\right] \quad (5.2.13a)$$

$$\frac{d\phi_3^e}{d\bar{x}} = -\frac{d\phi_1^e}{d\bar{x}} = \frac{6}{h_e}\frac{\bar{x}}{h_e}\left(1 - \frac{\bar{x}}{h_e}\right), \quad \frac{d\phi_4^e}{d\bar{x}} = -\frac{\bar{x}}{h_e}\left(3\frac{\bar{x}}{h_e} - 2\right)$$

$$\frac{d^2\phi_1^e}{d\bar{x}^2} = -\frac{6}{h_e^2}\left(1 - 2\frac{\bar{x}}{h_e}\right), \quad \frac{d^2\phi_2^e}{d\bar{x}^2} = -\frac{2}{h_e}\left(3\frac{\bar{x}}{h_e} - 2\right) \quad (5.2.13b)$$

$$\frac{d^2\phi_3^e}{d\bar{x}^2} = -\frac{d^2\phi_1^e}{d\bar{x}^2} = \frac{6}{h_e^2}\left(1 - 2\frac{\bar{x}}{h_e}\right), \quad \frac{d^2\phi_4^e}{d\bar{x}^2} = -\frac{2}{h_e}\left(3\frac{\bar{x}}{h_e} - 1\right)$$

$$\frac{d^3\phi_1^e}{d\bar{x}^3} = \frac{12}{h_e^3}, \quad \frac{d^3\phi_2^e}{d\bar{x}^3} = -\frac{6}{h_e^2}$$

$$\frac{d^3\phi_3^e}{d\bar{x}^3} = -\frac{12}{h_e^3}, \quad \frac{d^3\phi_4^e}{d\bar{x}^3} = -\frac{6}{h_e^2} \quad (5.2.13c)$$

Plots of  $d\phi_i^e/dx$  are shown in Fig. 5.2.5.

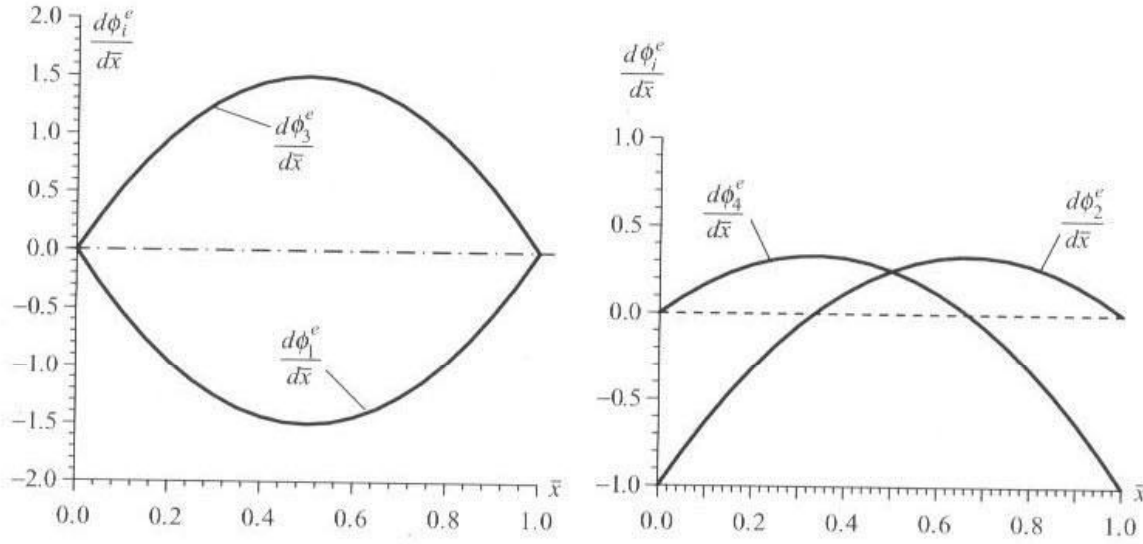


Figure 5.2.5 Plots of the first derivatives,  $d\phi_i^e/d\bar{x}$ , of the Hermite cubic interpolation functions.

The Hermite cubic interpolation functions (5.2.11) or (5.2.12) satisfy the following interpolations properties (see Figs. 5.2.4 and 5.2.5):

$$\begin{aligned}
 \phi_1^e(x_e) &= 1, & \phi_i^e(x_e) &= 0 \quad (i \neq 1) \\
 \phi_3^e(x_{e+1}) &= 1, & \phi_i^e(x_{e+1}) &= 0 \quad (i \neq 3) \\
 \left(-\frac{d\phi_2^e}{dx}\right)\bigg|_{x_e} &= 1, & \left(-\frac{d\phi_i^e}{dx}\right)\bigg|_{x_e} &= 0 \quad (i \neq 2) \\
 \left(-\frac{d\phi_4^e}{dx}\right)\bigg|_{x_{e+1}} &= 1, & \left(-\frac{d\phi_i^e}{dx}\right)\bigg|_{x_{e+1}} &= 0 \quad (i \neq 4)
 \end{aligned} \tag{5.2.14a}$$

These can be stated in compact form as ( $i, j = 1, 2$ )

$$\begin{aligned}
 \phi_{2i-1}^e(\bar{x}_j) &= \delta_{ij}, & \phi_{2i}^e(\bar{x}_j) &= 0, & \sum_{i=1}^2 \phi_{2i-1}^e &= 1 \\
 \left(\frac{d\phi_{2i-1}^e}{dx}\right)\bigg|_{\bar{x}_j} &= 0, & \left(-\frac{d\phi_{2i}^e}{dx}\right)\bigg|_{\bar{x}_j} &= \delta_{ij}
 \end{aligned} \tag{5.2.14b}$$

where  $\bar{x}_1 = 0$  and  $\bar{x}_2 = h_e$  are the local coordinates of nodes 1 and 2 of the element  $\Omega^e = (x_e, x_{e+1})$ . The finite element solution

$$w_h^e(x) = \Delta_1^e \phi_1^e(x) + \Delta_2^e \phi_2^e(x) + \Delta_3^e \phi_3^e(x) + \Delta_4^e \phi_4^e(x)$$

is a linear combination of four terms, which is shown in Fig. 5.2.6 along with the actual function.

It should be noted that the order of the interpolation functions derived above is the minimum required for the variational formulation (5.2.4). If a higher-order (i.e., higher than cubic) approximation of  $w$  is desired, we must either identify additional primary

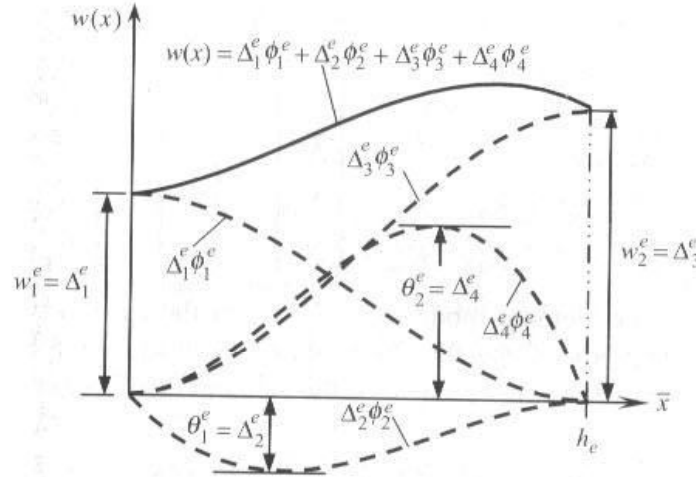


Figure 5.2.6 Finite element solution over an element.

unknowns at each of the two nodes or add additional nodes with the two degrees of freedom  $(w, -dw/dx)$ . For example, if we add  $d^2w/dx^2$  as the primary unknown at each of the two nodes or add a third node with  $(w, -dw/dx)$  at each node, there will be a total of six conditions, and a fifth-order polynomial is required to interpolate the end conditions (see Problems 5.4 and 5.5). However, interelement continuity of  $d^2w/dx^2$  (curvature) is not required by the weak form (5.2.4).

**Finite Element Model.** The finite element model of the Euler–Bernoulli beam is obtained by substituting the finite element interpolation (5.2.10) for  $w$  and the  $\phi_j^e$  for the weight function  $v$  into the weak form (5.2.4). Since there are four nodal variables  $\Delta_i^e$ , four different choices are used for  $v$ :  $v = \phi_1^e, \phi_2^e, \phi_3^e$ , and  $\phi_4^e$ , allowing us to obtain a set of four algebraic equations. The  $i$ th algebraic equation of the finite element model is (for  $v = \phi_i^e$ )

$$0 = \sum_{j=1}^4 \left[ \int_{x_e}^{x_{e+1}} \left( EI \frac{d^2 \phi_i^e}{dx^2} \frac{d^2 \phi_j^e}{dx^2} + c_f \phi_i^e \phi_j^e \right) dx \right] u_j^e - \int_{x_e}^{x_{e+1}} \phi_i^e q dx - Q_i^e \quad (5.2.15a)$$

or

$$\sum_{j=1}^4 K_{ij}^e \Delta_j^e - F_i^e = 0 \quad \text{or} \quad [K^e] \{\Delta^e\} = \{F^e\} \quad (5.2.15b)$$

where

$$K_{ij}^e = \int_{x_e}^{x_{e+1}} \left( EI \frac{d^2 \phi_i^e}{dx^2} \frac{d^2 \phi_j^e}{dx^2} + c_f \phi_i^e \phi_j^e \right) dx \quad (5.2.16a)$$

$$F_i^e = \int_{x_e}^{x_{e+1}} \phi_i^e q dx + Q_i^e \quad (5.2.16b)$$

Note that the coefficients  $K_{ij}^e$  are symmetric:  $K_{ij}^e = K_{ji}^e$ . In matrix notation, (5.2.15b) can be written as

$$\begin{bmatrix} K_{11}^e & K_{12}^e & K_{13}^e & K_{14}^e \\ K_{21}^e & K_{22}^e & K_{23}^e & K_{24}^e \\ K_{31}^e & K_{32}^e & K_{33}^e & K_{34}^e \\ K_{41}^e & K_{42}^e & K_{43}^e & K_{44}^e \end{bmatrix} \begin{Bmatrix} \Delta_1^e \\ \Delta_2^e \\ \Delta_3^e \\ \Delta_4^e \end{Bmatrix} = \begin{Bmatrix} q_1^e \\ q_2^e \\ q_3^e \\ q_4^e \end{Bmatrix} + \begin{Bmatrix} Q_1^e \\ Q_2^e \\ Q_3^e \\ Q_4^e \end{Bmatrix} \quad (5.2.17)$$

This represents the finite element model of (5.2.1). For the case in which  $EI$  and  $q$  are constant over an element, the element stiffness matrix  $[K^e]$  and force vector  $\{F^e\}$  have the following specific forms [see Fig. 5.2.2(c) for the element displacement and force degrees of freedom]

$$[K^e] = \frac{2E_e I_e}{h_e^3} \begin{bmatrix} 6 & -3h_e & -6 & -3h_e \\ -3h_e & 2h_e^2 & 3h_e & h_e^2 \\ -6 & 3h_e & 6 & 3h_e \\ -3h_e & h_e^2 & 3h_e & 2h_e^2 \end{bmatrix} + \frac{c_f^e h_e}{420} \begin{bmatrix} 156 & -22h_e & 54 & 13h_e \\ -22h_e & 4h_e^2 & -13h_e & -3h_e^2 \\ 54 & -13h_e & 156 & 22h_e \\ 13h_e & -3h_e^2 & 22h_e & 4h_e^2 \end{bmatrix}$$

$$\{F^e\} = \frac{q_e h_e}{12} \begin{Bmatrix} 6 \\ -h_e \\ 6 \\ h_e \end{Bmatrix} + \begin{Bmatrix} Q_1 \\ Q_2 \\ Q_3 \\ Q_4 \end{Bmatrix} \quad (5.2.18)$$

It can be verified that the generalized force vector in (5.2.18) represents the “statically equivalent” forces and moments at nodes 1 and 2 due to the uniformly distributed load of intensity  $q_e$  over the element (see Fig. 5.2.7). For any given function  $q(x)$ , (5.2.16b) provides a straightforward way of computing the components of the generalized force vector  $\{q^e\}$

$$q_i^e = \int_{x_e}^{x_{e+1}} \phi_i^e q \, dx \quad (5.2.19)$$

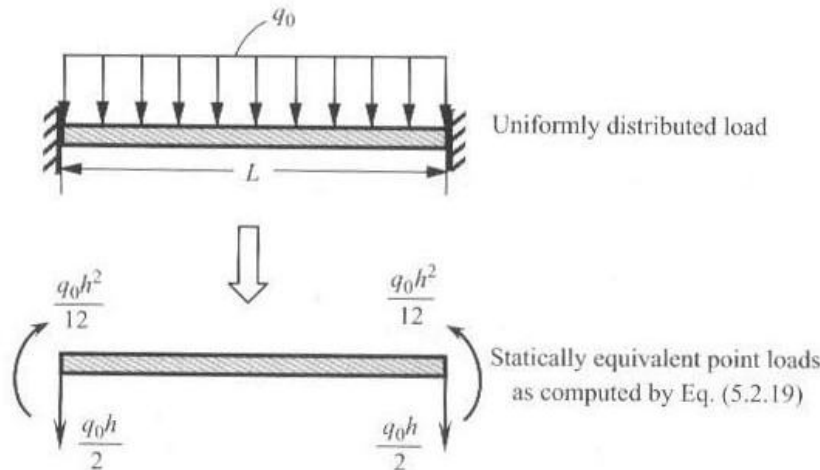


Figure 5.2.7 Generalized nodal forces due to uniformly distributed load.

When a transverse point force  $F_0^e$  is applied at a point  $x_0$  inside the element, it is distributed to the element nodes by the relation [see Remark 5 in Chapter 3; Eq. (3.3.4)]:

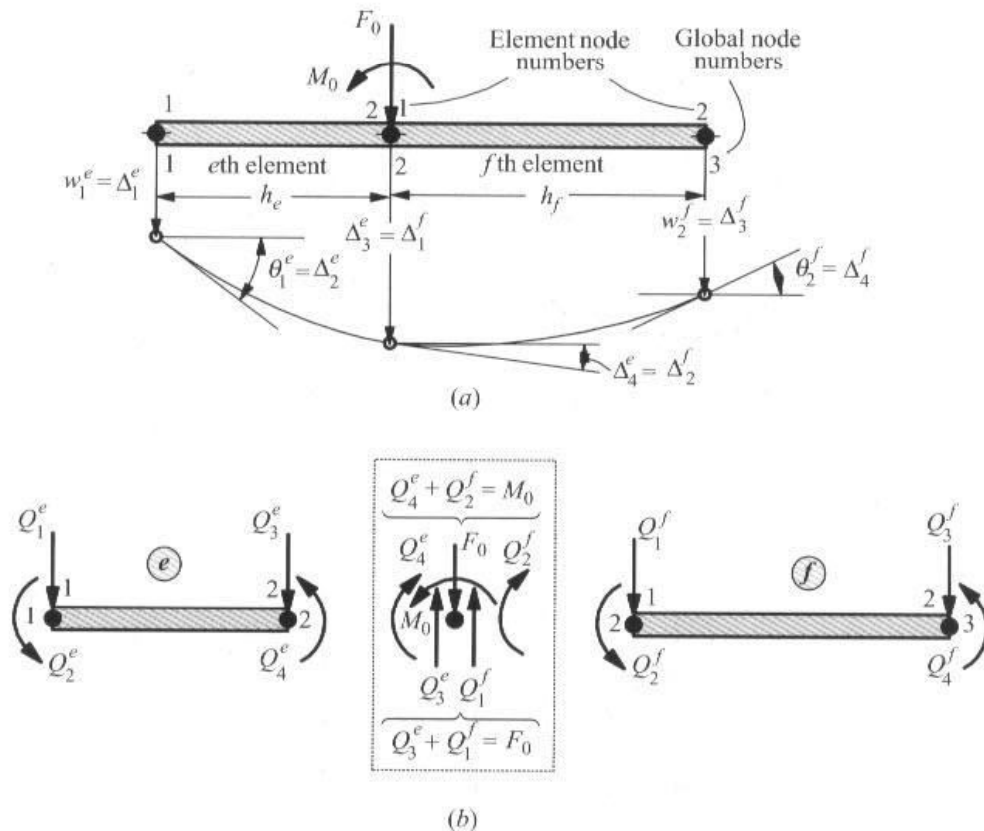
$$q_i^e = \int_{x_e}^{x_{e+1}} \phi_i^e(x) F_0^e \delta(x - x_0) dx = F_0^e \phi_i^e(x_0), \quad x_e \leq x_0 \leq x_{e+1} \quad (5.2.20)$$

which contains both transverse forces ( $q_1^e$  and  $q_3^e$ ) and bending moments ( $q_2^e$  and  $q_4^e$ ).

#### 5.2.4 Assembly of Element Equations

The assembly procedure for beam elements is the same as that used for bar elements except that we must take into account the two degrees of freedom at each node. Recall that the assembly of elements is based on: (a) interelement continuity of the primary variables (deflection and slope) and (b) interelement equilibrium of the secondary variable (shear force and bending moment) at the nodes common to elements. To demonstrate the assembly procedure, we select a two-element model (see Fig. 5.2.8). There are three global nodes and a total of six global generalized displacements and six generalized forces in the problem. The continuity of the primary variables implies the following relation between the element degrees of freedom  $\Delta_i^e$  and the global degrees of freedom  $U_i$  (see Fig. 5.2.8):

$$\begin{aligned} \Delta_1^1 &= U_1, & \Delta_2^1 &= U_2, & \Delta_3^1 &= \Delta_1^2 = U_3 \\ \Delta_4^1 &= \Delta_2^2 = U_4, & \Delta_3^2 &= U_5, & \Delta_4^2 &= U_6 \end{aligned} \quad (5.2.21)$$



**Figure 5.2.8** Assembly of two Euler-Bernoulli beam finite elements. (a) Continuity of generalized displacements. (b) Balance of the generalized forces.

In general, the equilibrium of the generalized forces at a node between two connecting elements  $\Omega_e$  and  $\Omega_f$  requires that

$$\begin{aligned} Q_3^e + Q_1^f &= \text{applied external point force} \\ Q_4^e + Q_2^f &= \text{applied external bending moment} \end{aligned} \quad (5.2.22)$$

If no external applied forces are given, the sum should be equated to zero. In equating the sums to the applied generalized forces (i.e., force or moment), the sign convention for the element force degrees of freedom [see Fig. 5.2.2(c)] should be followed. Forces are taken as positive when they act in the direction of positive  $z$ -axis, and moments are taken as positive when they follow the right-hand screw rule (i.e., when the thumb is along the positive  $y$ -axis, the four fingers show the direction of the moment). With respect to the coordinate system used in Figs. 5.2.1 and 5.2.2, *forces acting downward are positive and counterclockwise moments are positive.*

To impose the equilibrium of forces in (5.2.22), it is necessary to add the third and fourth equations (corresponding to the second node) of element  $\Omega^e$  to the first and second equations (corresponding to the first node) of element  $\Omega^f$ . Consequently, the global stiffness parameters  $K_{33}$ ,  $K_{34}$ ,  $K_{43}$ , and  $K_{44}$  associated with global node 2 are the superposition of the element stiffnesses:

$$K_{33} = K_{33}^1 + K_{11}^2, \quad K_{34} = K_{34}^1 + K_{12}^2, \quad K_{43} = K_{43}^1 + K_{21}^2, \quad K_{44} = K_{44}^1 + K_{22}^2 \quad (5.2.23)$$

In general, the assembled stiffness matrix and force vector for beam elements connected in series have the forms given in Eqs. (5.2.24a) and (5.2.24b):

$$[K] = \begin{array}{c} \begin{array}{cc|cc|cc} \text{Global node 1} & & \text{Global node 2} & & \text{Global node 3} & \\ \hline K_{11}^1 & K_{12}^1 & K_{13}^1 & K_{14}^1 & & \\ K_{21}^1 & K_{22}^1 & K_{23}^1 & K_{24}^1 & & \\ \hline K_{31}^1 & K_{32}^1 & K_{33}^1 + K_{11}^2 & K_{34}^1 + K_{12}^2 & K_{13}^2 & K_{14}^2 \\ K_{41}^1 & K_{42}^1 & K_{43}^1 + K_{21}^2 & K_{44}^1 + K_{22}^2 & K_{23}^2 & K_{24}^2 \\ \hline & & K_{31}^2 & K_{32}^2 & K_{33}^2 & K_{34}^2 \\ & & K_{41}^2 & K_{42}^2 & K_{43}^2 & K_{44}^2 \end{array} & \left. \begin{array}{l} \} 1 \\ \} 2 \\ \} 3 \end{array} \right\} \end{array} \quad (5.2.24a)$$

$$\{F\} = \begin{Bmatrix} q_1^1 \\ q_2^1 \\ q_3^1 + q_1^2 \\ q_4^1 + q_2^2 \\ q_3^2 \\ q_4^2 \end{Bmatrix} + \begin{Bmatrix} Q_1^1 \\ Q_2^1 \\ Q_3^1 + Q_1^2 \\ Q_4^1 + Q_2^2 \\ Q_3^2 \\ Q_4^2 \end{Bmatrix} \quad (5.2.24b)$$


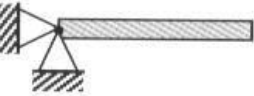



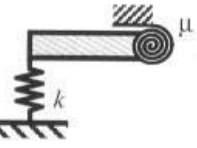
### 5.2.5 Imposition of Boundary Conditions

At this step of the analysis, we must impose the particular boundary conditions of the problem being analyzed. The type of essential (also known as *geometric*) boundary conditions for a specific beam problem depend on the nature of the geometric support. Table 5.2.1 contains a list of commonly used geometric supports for beams. The natural (also called *force*) boundary conditions involve the specification of generalized forces when the corresponding primary variables are not constrained. One must bear in mind that one and only one element of each of the following pairs must be specified at every node of the finite element mesh:

$$\left( w, \frac{d}{dx} \left[ EI \frac{d^2 w}{dx^2} \right] \right), \left( \frac{dw}{dx}, EI \frac{d^2 w}{dx^2} \right) \quad (5.2.25)$$

At an interior node, we impose the continuity of generalized displacements and balance of generalized forces as discussed in Eqs. (5.2.21) and (5.2.22).

**Table 5.2.1** Types of commonly used support conditions for beams and frames.

Type of support	Displacement boundary conditions	Force boundary conditions
Free 	None	All, as specified
Pinned 	$u = 0$ $w = 0$	Moment is specified
Roller (vertical) 	$u = 0$	Transverse force and moment are specified
Roller (horizontal) 	$w = 0$	Horizontal force and bending moment are specified
Fixed (or clamped) 	$u = 0$ $w = 0$ $dw/dx = 0$	None specified
Elastically restrained 	$EI(d^2w/dx^2) + \mu\theta = M_0, M_0 \text{ specified}$ $EI(d^3w/dx^3) + kw = Q_0, Q_0 \text{ specified}$	

There are two alternative ways to include the effect of a linear elastic spring (extensional as well as torsional). (1) Include the spring through the boundary condition for the appropriate degree of freedom (see Table 5.2.1). (2) Include the spring as another finite element, whose element equations are given by Eq. (4.2.2). In the former case, after assembly of the element equations, the secondary variable in the direction of the spring action is replaced by the negative of the spring constant times the associated primary variable. Let  $Q^v$ , and  $Q^\theta$  denote the secondary variables associated with the transverse and rotational degrees of freedom at a node. Then, we have, respectively

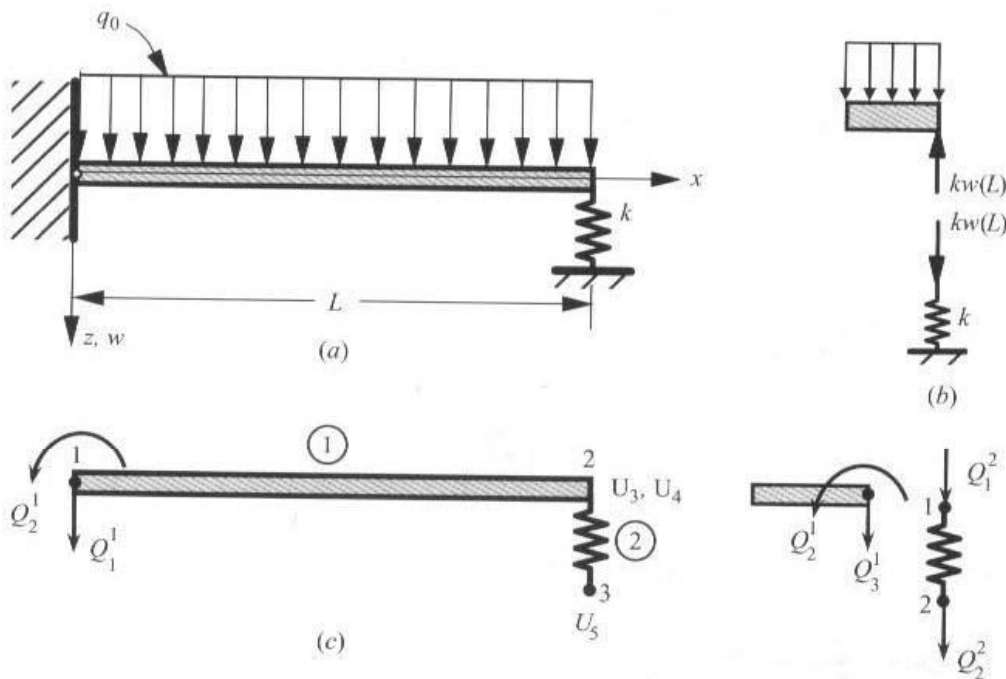
$$Q^v + kw = 0 \text{ or } Q^v = -kw \text{ for vertical spring with spring constant } k$$

$$Q^\theta + \mu\theta = 0 \text{ or } Q^\theta = -\mu\theta \text{ for torsional spring with spring constant } \mu$$

Note that  $Q^v$  is the shear force and  $Q^\theta$  the bending moment. In the second case, the spring element may be assembled along with beam elements by noting that the axial displacement of the spring is the same as the transverse displacement of the beam.

For example, consider the case of a beam clamped at the left end and supported by a spring at the right end, as shown in Fig. 5.2.9(a). Using one-element model of the beam, we obtain [set  $c_f = 0$  in Eq. (5.2.18)]

$$\frac{2EI}{L^3} \begin{bmatrix} 6 & -3L & -6 & -3L \\ -3L & 2L^2 & 3L & L^2 \\ -6 & 3L & 6 & 3L \\ -3L & L^2 & 3L & 2L^2 \end{bmatrix} \begin{Bmatrix} U_1 \\ U_2 \\ U_3 \\ U_4 \end{Bmatrix} = \frac{q_0 L}{12} \begin{Bmatrix} 6 \\ -L \\ 6 \\ L \end{Bmatrix} + \begin{Bmatrix} Q_1 \\ Q_2 \\ Q_3 \\ Q_4 \end{Bmatrix}$$



**Figure 5.2.9** (a) A spring supported cantilever beam. (b) Spring action. (c) Finite element mesh of beam and spring elements.

The obvious boundary conditions are  $U_1 = U_2 = Q_4 = 0$ . The effect of the spring is that [see Fig. 5.2.9(b)] it exerts a force of  $kU_3$  upward on the beam. Hence,  $Q_3 = -kU_3$ . Thus, we have

$$\frac{2EI}{L^3} \begin{bmatrix} 6 & -3L & -6 & -3L \\ -3L & 2L^2 & 3L & L^2 \\ -6 & 3L & 6 & 3L \\ -3L & L^2 & 3L & 2L^2 \end{bmatrix} \begin{Bmatrix} 0 \\ 0 \\ U_3 \\ U_4 \end{Bmatrix} = \frac{q_0 L}{12} \begin{Bmatrix} 6 \\ -L \\ 6 \\ L \end{Bmatrix} + \begin{Bmatrix} Q_1 \\ Q_2 \\ -kU_3 \\ 0 \end{Bmatrix}$$

and the condensed equations for the unknown displacements  $U_3$  (deflection) and  $U_4$  (rotation) become

$$\begin{bmatrix} \frac{12EI}{L^3} + k & \frac{6EI}{L^2} \\ \frac{6EI}{L^2} & \frac{4EI}{L} \end{bmatrix} \begin{Bmatrix} U_3 \\ U_4 \end{Bmatrix} = \frac{q_0 L}{12} \begin{Bmatrix} 6 \\ L \end{Bmatrix}$$

whose solution is

$$U_3 = w(L) = \frac{q_0 L^4}{8EI} \frac{1}{\left(1 + \frac{kL^3}{3EI}\right)}, \quad U_4 = \theta(L) = -\frac{q_0 L^3}{6EI} \frac{\left(EI - \frac{kL^3}{24}\right)}{\left(EI + \frac{kL^3}{3}\right)}$$

Note that when  $k = 0$ , we obtain the deflection  $U_3 = q_0 L^4 / 8EI$  and rotation  $U_4 = -q_0 L^3 / 6EI$  at the free end of a cantilever beam under uniformly distributed load of intensity  $q_0$ . When  $k \rightarrow \infty$ , we obtain the deflection  $U_3 = 0$  and rotation  $U_4 = -q_0 L^3 / 48EI$  at  $x = L$  (where it is simply supported).

Alternatively, the assembly of the beam and spring elements [see Fig. 5.2.9(c)] yields the result

$$\begin{bmatrix} \frac{12EI}{L^3} & -\frac{6EI}{L^2} & -\frac{12EI}{L^3} & -\frac{6EI}{L^2} & 0 \\ -\frac{6EI}{L^2} & \frac{4EI}{L} & \frac{6EI}{L^2} & \frac{2EI}{L} & 0 \\ -\frac{12EI}{L^3} & \frac{6EI}{L^2} & \frac{12EI}{L^3} + k & \frac{6EI}{L^2} & -k \\ -\frac{6EI}{L^2} & \frac{2EI}{L} & \frac{6EI}{L^2} & \frac{4EI}{L} & 0 \\ 0 & 0 & -k & 0 & k \end{bmatrix} \begin{Bmatrix} U_1 \\ U_2 \\ U_3 \\ U_4 \\ U_5 \end{Bmatrix} = \frac{q_0 L}{12} \begin{Bmatrix} 6 \\ -L \\ 6 \\ L \\ 0 \end{Bmatrix} + \begin{Bmatrix} Q_1^1 \\ Q_2^1 \\ Q_3^1 + Q_1^2 \\ Q_4^1 \\ Q_2^2 \end{Bmatrix}$$

Using the boundary conditions,  $U_1 = U_2 = U_5 = 0$  and  $Q_4^1 = 0$ , and the equilibrium condition  $Q_3^1 + Q_1^2 = 0$ , we obtain the condensed equations

$$\begin{bmatrix} \frac{12EI}{L^3} + k & \frac{6EI}{L^2} \\ \frac{6EI}{L^2} & \frac{4EI}{L} \end{bmatrix} \begin{Bmatrix} U_3 \\ U_4 \end{Bmatrix} = \frac{q_0 L}{12} \begin{Bmatrix} 6 \\ L \end{Bmatrix}$$

which are identical to those obtained earlier.

### 5.2.6 Postprocessing of the Solution

Once the boundary conditions are imposed, the resulting equations are solved for the unknown nodal displacements and forces. The solution is then given by Eq. (5.2.10) in each

element. The slope of the deflection at an interior point is

$$-\frac{dw_h^e}{dx} = -\sum_{j=1}^4 \Delta_j^e \frac{d\phi_j^e}{dx} \quad (5.2.26)$$

Similarly, the bending moment at any point in the element  $\Omega^e$  of the beam can be computed from the formula

$$\begin{aligned} M(x) &= \int_A \sigma_x z dA = B \int_{-H/2}^{H/2} \sigma_x z dz = -BE \int_{-H/2}^{H/2} z^2 \frac{d^2 w}{dx^2} dz = -EI \frac{d^2 w}{dx^2} \\ &= -EI \sum_{j=1}^4 \Delta_j^e \frac{d^2 \phi_j^e}{dx^2} \end{aligned} \quad (5.2.27)$$

where  $B$  is the width and  $H$  is the height of the beam (for a rectangular cross-section beam). The bending stress is given by

$$\sigma_x(x, z) = -\frac{M(x)z}{I} = Ez \frac{d^2 w}{dx^2} = Ez \sum_{j=1}^4 \Delta_j^e \frac{d^2 \phi_j^e(x)}{dx^2} \quad (5.2.28)$$

The maximum tensile stress occurs at the bottom ( $z = H/2$ ) and the maximum compressive stress at the top ( $z = -H/2$ ) of the beam.

We close this section with a note that whenever the flexural rigidity  $EI$  is a constant in each element, the finite element solution for the generalized displacements at the nodes is exact for any applied transverse load  $q$ . Further, the solution is exact at all points if the distributed load is such that the exact solution is a cubic.

### 5.2.7 Numerical Examples

#### Example 5.2.1

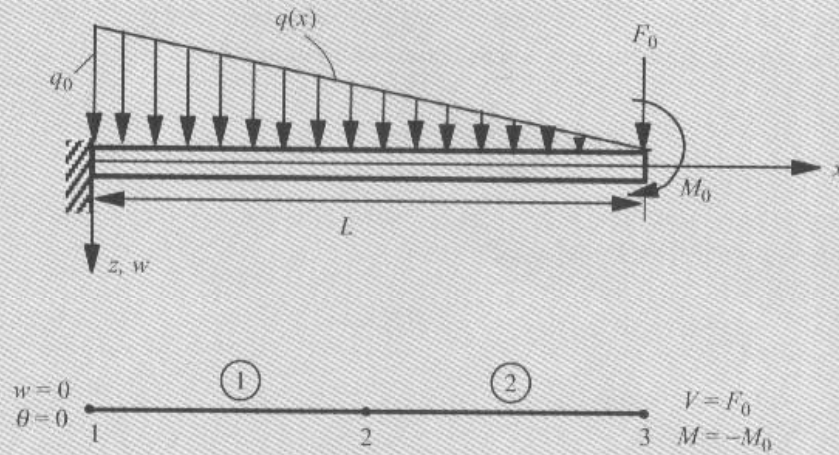
Consider a cantilever beam of length  $L$  and subjected to linearly varying distributed load  $q(x)$ , point load  $F_0$ , and moment  $M_0$ , as shown in Fig. 5.2.10. We wish to determine the displacement field and bending moment in the beam using two elements ( $h = L/2$ ).

First we note that  $q(x) = q_0(1 - x/L)$ . There, we must evaluate its contribution to the element load vector by computing [see Eq. (5.2.19)]

$$q_i^e = \int_{x_e}^{x_{e+1}} q_0 \left(1 - \frac{x}{L}\right) \phi_i^e(x) dx = \int_0^{h_e} q_0 \left(1 - \frac{\bar{x} + x_e}{L}\right) \phi_i^e(\bar{x}) d\bar{x}$$

where  $\phi_i^e(\bar{x})$  are given in Eq. (5.2.12). Evaluating the integrals,

$$\{q^e\} = \frac{q_0 h_e}{12} \begin{Bmatrix} 6 \\ -h_e \\ 6 \\ h_e \end{Bmatrix} + \frac{q_0 h_e}{60L} \begin{Bmatrix} -(9h_e + 30x_e) \\ h_e(2h_e + 5x_e) \\ -(21h_e + 30x_e) \\ -h_e(3h_e + 5x_e) \end{Bmatrix}$$



**Figure 5.2.10** The cantilever beam problem considered in Example 5.2.1.

and specializing the above vectors to element 1 ( $x_e = 0$ ) and element 2 ( $x_e = h_e$ ), we obtain

$$\{q^1\} = \frac{q_0 L}{48} \begin{Bmatrix} 12 \\ -L \\ 12 \\ L \end{Bmatrix} + \frac{q_0 L^2}{480} \begin{Bmatrix} -18 \\ 2L \\ -42 \\ -3L \end{Bmatrix}; \{q^2\} = \frac{q_0 L}{48} \begin{Bmatrix} 12 \\ -L \\ 12 \\ L \end{Bmatrix} + \frac{q_0 L^2}{480} \begin{Bmatrix} -78 \\ 7L \\ -102 \\ -8L \end{Bmatrix}$$

The assembled system of equations for a mesh of two elements with constant  $EI$  (and foundation modulus  $c_f = 0$ ) is

$$\frac{2EI}{h^3} \begin{bmatrix} 6 & -3h & -6 & -3h & 0 & 0 \\ -3h & 2h^2 & 3h & h^2 & 0 & 0 \\ -6 & 3h & 6+6 & 3h-3h & -6 & -3h \\ -3h & h^2 & 3h-3h & 2h^2+2h^2 & 3h & h^2 \\ 0 & 0 & -6 & 3h & 6 & 3h \\ 0 & 0 & -3h & h^2 & 3h & 2h^2 \end{bmatrix} \begin{Bmatrix} U_1 \\ U_2 \\ U_3 \\ U_4 \\ U_5 \\ U_6 \end{Bmatrix} = \frac{q_0 L}{48} \begin{Bmatrix} 12 \\ -L \\ 24 \\ 0 \\ 12 \\ L \end{Bmatrix} + \frac{q_0 L}{480} \begin{Bmatrix} -18 \\ 2L \\ -120 \\ 4L \\ -102 \\ -8L \end{Bmatrix} + \begin{Bmatrix} Q_1^1 \\ Q_2^1 \\ Q_3^1 + Q_1^2 \\ Q_4^1 + Q_2^2 \\ Q_3^2 \\ Q_4^2 \end{Bmatrix}$$

At global node 1,  $Q_1^1$  and  $Q_2^1$  (the shear force and the bending moment, respectively), i.e., the reactions at the fixed end are not known. Hence, the corresponding generalized displacements,

$U_1$  and  $U_2$  must be known. Since the end  $x = 0$  is fixed, we have  $U_1 = U_2 = 0$ . At global node 2, there are no externally applied shear forces and bending moment, i.e.,

$$Q_3^1 + Q_1^2 = 0, \quad Q_4^1 + Q_2^2 = 0$$

At global node 3, the shear force is given as  $F_0$ , and the bending moment as  $M_0$  [note the sign convention for  $F_0$  and  $M_0$  from Fig. 5.2.2(c)]:

$$Q_3^2 = F_0, \quad Q_4^2 = -M_0$$

Hence, the assembled equations take the form

$$\begin{aligned} \frac{4EI}{L^3} \begin{bmatrix} 24 & -6L & -24 & -6L & 0 & 0 \\ -6L & 2L^2 & 6L & L^2 & 0 & 0 \\ -24 & 6L & 48 & 0 & -24 & -6L \\ -6L & L^2 & 0 & 4L^2 & 6L & L^2 \\ 0 & 0 & -24 & 6L & 24 & 6L \\ 0 & 0 & -6L & L^2 & 6L & 2L^2 \end{bmatrix} \begin{Bmatrix} 0 \\ 0 \\ U_3 \\ U_4 \\ U_5 \\ U_6 \end{Bmatrix} \\ = \frac{q_0 L}{48} \begin{Bmatrix} 12 \\ -L \\ 24 \\ 0 \\ 12 \\ L \end{Bmatrix} + \frac{q_0 L}{480} \begin{Bmatrix} -18 \\ 2L \\ -120 \\ 4L \\ -102 \\ -8L \end{Bmatrix} + \begin{Bmatrix} Q_1^1 \\ Q_2^1 \\ 0 \\ 0 \\ F_0 \\ -M_0 \end{Bmatrix} \end{aligned}$$

Thus, the condensed equations for the unknown generalized displacements and generalized forces are

$$\begin{aligned} \frac{4EI}{L^3} \begin{bmatrix} 48 & 0 & -24 & -6L \\ 0 & 4L^2 & 6L & L^2 \\ -24 & 6L & 24 & 6L \\ -6L & L^2 & 6L & 2L^2 \end{bmatrix} \begin{Bmatrix} U_3 \\ U_4 \\ U_5 \\ U_6 \end{Bmatrix} = \frac{q_0 L}{48} \begin{Bmatrix} 24 \\ 0 \\ 12 \\ L \end{Bmatrix} + \frac{q_0 L}{480} \begin{Bmatrix} -120 \\ 4L \\ -102 \\ -8L \end{Bmatrix} + \begin{Bmatrix} 0 \\ 0 \\ F_0 \\ -M_0 \end{Bmatrix} \\ \begin{Bmatrix} Q_1^1 \\ Q_2^1 \end{Bmatrix} = \frac{4EI}{L^3} \begin{bmatrix} -24 & -6L & 0 & 0 \\ 6L & L^2 & 0 & 0 \end{bmatrix} \begin{Bmatrix} U_3 \\ U_4 \\ U_5 \\ U_6 \end{Bmatrix} - \frac{q_0 L}{48} \begin{Bmatrix} 12 \\ -L \end{Bmatrix} - \frac{q_0 L}{480} \begin{Bmatrix} -18 \\ 2L \end{Bmatrix} \end{aligned}$$

The solution of the condensed equations for the displacements yields

$$\begin{aligned}
 \begin{Bmatrix} U_3 \\ U_4 \\ U_5 \\ U_6 \end{Bmatrix} &= \frac{L^3}{4EI} \begin{bmatrix} 48 & 0 & -24 & -6L \\ 0 & 4L^2 & 6L & L^2 \\ -24 & 6L & 24 & 6L \\ -6L & L^2 & 6L & 2L^2 \end{bmatrix}^{-1} \begin{Bmatrix} \frac{1}{4}q_0L \\ \frac{1}{120}q_0L^2 \\ F_0 + \frac{3}{80}q_0L \\ -M_0 + \frac{1}{240}q_0L^2 \end{Bmatrix} \\
 &= \frac{L}{48EI} \begin{bmatrix} 2L^2 & -6L & 5L^2 & -6L \\ -6L & 24 & -18L & 24 \\ 5L^2 & -18L & 16L^2 & -24L \\ -6L & 24 & -24L & 48 \end{bmatrix} \begin{Bmatrix} \frac{1}{4}q_0L \\ \frac{1}{120}q_0L^2 \\ F_0 + \frac{3}{80}q_0L \\ -M_0 + \frac{1}{240}q_0L^2 \end{Bmatrix} \\
 &= \frac{L}{48EI} \begin{Bmatrix} 5L^2F_0 + 6LM_0 + \frac{49}{80}q_0L^3 \\ -18LF_0 - 24M_0 - \frac{15}{8}q_0L^2 \\ 16L^2F_0 + 24LM_0 + \frac{16}{10}q_0L^3 \\ -24LF_0 - 48M_0 - 2q_0L^2 \end{Bmatrix} \quad (5.2.29)
 \end{aligned}$$

The reactions  $Q_1^1$  and  $Q_2^1$  are

$$\begin{Bmatrix} Q_1^1 \\ Q_2^1 \end{Bmatrix} = \frac{4EI}{L^3} \begin{bmatrix} -24 & -6L \\ 6L & L^2 \end{bmatrix} \begin{Bmatrix} U_3 \\ U_4 \end{Bmatrix} - \frac{q_0L}{480} \begin{Bmatrix} 102 \\ -8L \end{Bmatrix} = \begin{Bmatrix} -(F_0 + \frac{1}{2}q_0L) \\ L(F_0 + \frac{1}{6}q_0L) + M_0 \end{Bmatrix} \quad (5.2.30)$$

It is clear that the reactions  $Q_1^1$  and  $Q_2^1$  computed above satisfy the static equilibrium equations of the beam:

$$Q_1^1 + F_0 + \frac{1}{2}q_0L = 0, \quad Q_2^1 - \left( F_0L + \frac{1}{6}q_0L^2 + M_0 \right) = 0$$

The reactions  $Q_1^1$  and  $Q_2^1$  can also be computed using the definitions (5.2.3):

$$(Q_1^1)_{\text{def}} = \frac{d}{dx} \left( EI \frac{d^2w}{dx^2} \right) \Big|_{x=0}, \quad (Q_2^1)_{\text{def}} = \left( EI \frac{d^2w}{dx^2} \right) \Big|_{x=0}$$

From (5.2.13b) and (5.2.13c), we note that the second derivative of the Hermite cubic interpolation functions is linear over the element and the third derivative is constant over the element. Therefore, the bending moment and shear force computed using the definition (5.2.3) are elementwise linear and constant, respectively. Further, at nodes connecting two elements, they yield discontinuous values because the second and third derivatives of  $w$  are not made continuous across the interelement nodes. Thus, we have

$$\begin{aligned}
 (Q_1^1)_{\text{def}} &= EI \left( U_3 \frac{d^3\phi_3^1}{dx^3} + U_4 \frac{d^3\phi_4^1}{dx^3} \right) \Big|_{x=0} = EI \left[ U_3 \left( -\frac{96}{L^3} \right) + U_4 \left( -\frac{24}{L^2} \right) \right] \\
 &= - \left( F_0 + \frac{23}{80}q_0L \right) \\
 (Q_2^1)_{\text{def}} &= EI \left( U_3 \frac{24}{L^2} + U_4 \frac{4}{L} \right) = \left( M_0 + F_0L + \frac{3}{20}q_0L^2 \right)
 \end{aligned}$$

which are in error by  $q_1^e = -\frac{17}{80}q_0L$  and  $q_2^e = \frac{1}{60}q_0L^2$  compared with those computed using the condensed (i.e., equilibrium) equations [see Eq. (5.2.30)].

The finite element solution as a function of position  $x$  is given by

$$w_h^e(x) = \begin{cases} U_3\phi_3^1 + U_4\phi_4^1 & \text{for } 0 \leq x \leq h \\ U_3\phi_1^2 + U_4\phi_2^2 + U_5\phi_3^2 + U_6\phi_4^2 & \text{for } h \leq x \leq 2h \end{cases} \quad (5.2.31a)$$

where

$$\begin{aligned} \phi_3^1 &= 3\left(\frac{x}{h}\right)^2 - 2\left(\frac{x}{h}\right)^3, & \phi_4^1 &= h\left[\left(\frac{x}{h}\right)^2 - \left(\frac{x}{h}\right)^3\right] \\ \phi_1^2 &= 1 - 3\left(1 - \frac{x}{h}\right)^2 - 2\left(1 - \frac{x}{h}\right)^3, & \phi_2^2 &= h\left(1 - \frac{x}{h}\right)\left(2 - \frac{x}{h}\right)^2 \\ \phi_3^2 &= 3\left(1 - \frac{x}{h}\right)^2 + 2\left(1 - \frac{x}{h}\right)^3, & \phi_4^2 &= h\left[\left(1 - \frac{x}{h}\right)^3 + \left(1 - \frac{x}{h}\right)^2\right] \end{aligned} \quad (5.2.31b)$$

The exact solution of the problem in Fig. 5.2.9 can be obtained by direct integration and is given by

$$\begin{aligned} w(x) &= \frac{q_0L^4}{120EI} \left[ 10\left(\frac{x}{L}\right)^2 - 10\left(\frac{x}{L}\right)^3 + 5\left(\frac{x}{L}\right)^4 - \left(\frac{x}{L}\right)^5 \right] \\ &\quad + \frac{F_0L^3}{6EI} \left[ -\left(\frac{x}{L}\right)^3 + 3\left(\frac{x}{L}\right)^2 \right] + \frac{M_0L^2}{2EI} \left(\frac{x}{L}\right)^2 \\ \theta(x) &= -\frac{q_0L^3}{24EI} \left[ 4\left(\frac{x}{L}\right) - 6\left(\frac{x}{L}\right)^2 + 4\left(\frac{x}{L}\right)^3 - \left(\frac{x}{L}\right)^4 \right] \\ &\quad + \frac{F_0L^2}{2EI} \left[ \left(\frac{x}{L}\right)^2 - 2\left(\frac{x}{L}\right) \right] - \frac{M_0}{EI} \left(\frac{x}{L}\right) \\ M(x) &= -\frac{q_0L^2}{6} \left[ 1 - 3\left(\frac{x}{L}\right) + 3\left(\frac{x}{L}\right)^2 - \left(\frac{x}{L}\right)^3 \right] + F_0L \left[ \left(\frac{x}{L}\right) - 1 \right] - M_0 \end{aligned} \quad (5.2.32)$$

The finite element solution (5.2.31) and the exact solution (5.2.32) are compared in Table 5.2.2 for the data

$$\begin{aligned} q_0 &= 24 \text{ kN/m}, & F_0 &= 60 \text{ kN}, & L &= 3 \text{ m}, & M_0 &= 0 \text{ kN-m} \\ E &= 200 \times 10^6 \text{ kN/m}^2, & I &= 29 \times 10^6 \text{ mm}^4, & (EI &= 5800 \text{ kN-m}^2) \end{aligned} \quad (5.2.33)$$

As expected, the finite element solution for  $w$  and  $\theta$  coincides with the exact solution at the nodes. At points other than the nodes, the difference between the finite element and exact solutions is virtually negligible.

**Table 5.2.2** Comparison of the finite element method (FEM) solution with the exact solution of the cantilever beam of Example 5.2.1 (2 elements).

$x$ (m)	$w$ (m)		$-\theta = dw/dx$		$-M \times 10^{-6}$ (kN m)	
	FEM	Exact	FEM	Exact	FEM	Exact
0.0000	0.0000 <sup>†</sup>	0.0000	0.0000 <sup>†</sup>	0.0000	0.2124 <sup>†</sup>	0.2160
0.1875	0.0006	0.0006	0.0066	0.0067	0.1973	0.1984
0.3750	0.0025	0.0025	0.0128	0.0128	0.1821	0.1816
0.5625	0.0054	0.0054	0.0184	0.0185	0.1670	0.1656
0.7500	0.0093	0.0094	0.0235	0.0235	0.1519	0.1502
0.9375	0.0142	0.0142	0.0282	0.0282	0.1367	0.1354
1.1250	0.0199	0.0199	0.0324	0.0323	0.1216	0.1213
1.3125	0.0263	0.0263	0.0361	0.0360	0.1065	0.1077
1.5000	0.0333 <sup>†</sup>	0.0334	0.0393 <sup>†</sup>	0.0393	0.0913*	0.0945
1.6875	0.0410	0.0410	0.0421	0.0421	0.0814	0.0818
1.8750	0.0491	0.0491	0.0445	0.0446	0.0696	0.0694
2.0625	0.0577	0.0577	0.0466	0.0466	0.0579	0.0574
2.2500	0.0666	0.0666	0.0483	0.0483	0.0461	0.0456
2.4375	0.0758	0.0758	0.0496	0.0496	0.0344	0.0340
2.6250	0.0852	0.0852	0.0505	0.0505	0.0226	0.0226
2.8025	0.0947	0.0947	0.0510	0.0510	0.0109	0.0113
3.0000	0.1043 <sup>†</sup>	0.1042	0.0512 <sup>†</sup>	0.0512	-0.0009	0.0000

\* 0.0932 from the second element.

† Nodal values; all others are computed by interpolation.

**Example 5.2.2**

Consider the indeterminate beam shown in Fig. 5.2.11(a). We assume the following discontinuous data ( $c_f = 0$ ):

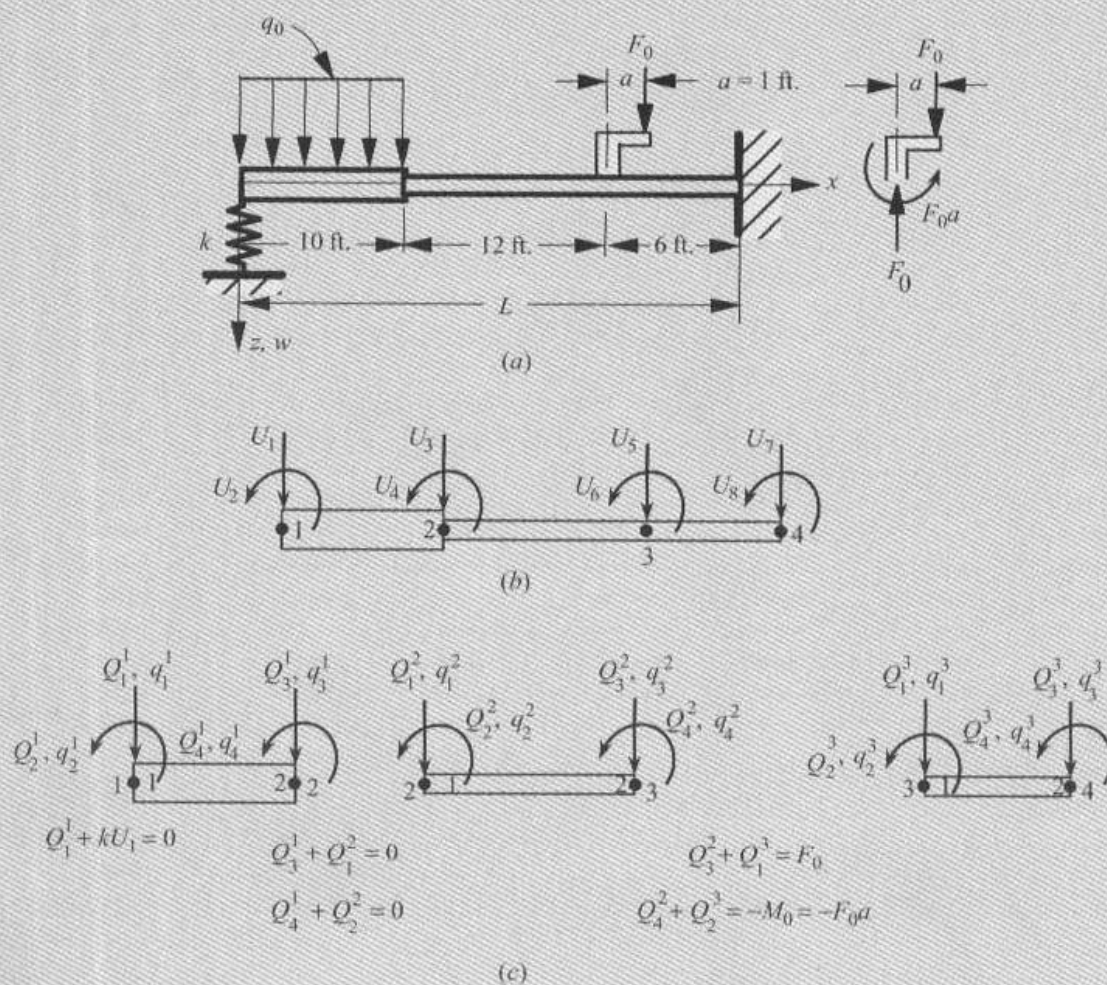
$$EI = \begin{cases} 2 \times 10^8 \text{ lb-ft.}^2 & \text{for } 0 \leq x \leq 10 \text{ ft.} \\ 10^8 \text{ lb-ft.}^2 & \text{for } 10 \leq x \leq 28 \text{ ft.} \end{cases} \quad (5.2.34a)$$

$$q(x) = \begin{cases} 2400 \text{ lb/ft.} & \text{for } 0 \leq x \leq 10 \text{ ft.} \\ 0 & \text{for } 10 \leq x \leq 28 \text{ ft.} \end{cases} \quad (5.2.34b)$$

The boundary conditions are

$$[EI(d^3w/dx^3) + kw]_{x=0} = 0, \quad [EI(d^2w/dx^2)]_{x=0} = 0, \quad w(28) = 0, \quad [dw/dx]_{x=28} = 0$$

We shall use three elements to analyze the problem. There are four nodes and eight global degrees of freedom in the nonuniform mesh of three elements.



**Figure 5.2.11** (a) Physical problem. (b) Finite element mesh of three elements. (c) Equilibrium of generalized forces.

Since  $ET$  and  $q$  are elementwise-constant, the element stiffness matrix and the force vector are given by (5.2.18), with  $q_e = 2400$  lb/ft. in element 1 and  $q_e = 0$  in elements 2 and 3. The assembled equations are

$$10^7 \begin{bmatrix} 0.2400 & -1.2000 & -0.2400 & -1.2000 & & & & \\ & 8.0000 & 1.2000 & 4.0000 & & & & \\ & & 0.3094 & 0.7833 & -0.0694 & -0.4167 & & \\ & & & 11.3333 & 0.4167 & 1.6667 & & \\ & & & & 0.6250 & -1.2500 & -0.5556 & -1.6667 \\ & & & & & 10.0000 & 1.6667 & 3.3333 \\ & & & & & & 0.5556 & 1.6667 \\ & & & & & & & 6.6667 \end{bmatrix} \begin{Bmatrix} U_1 \\ U_2 \\ U_3 \\ U_4 \\ U_5 \\ U_6 \\ U_7 \\ U_8 \end{Bmatrix} = \begin{Bmatrix} 0 \\ 0 \\ 0 \\ 0 \\ 0 \\ 0 \\ 0 \\ 0 \end{Bmatrix}$$

symmetric

$$\times \begin{Bmatrix} U_1 \\ U_2 \\ U_3 \\ U_4 \\ U_5 \\ U_6 \\ U_7 \\ U_8 \end{Bmatrix} = 10^3 \begin{Bmatrix} 12 \\ -20 \\ 12 \\ 20 \\ 0 \\ 0 \\ 0 \\ 0 \end{Bmatrix} + \begin{Bmatrix} Q_1^1 \\ Q_2^1 \\ Q_3^1 + Q_1^2 \\ Q_4^1 + Q_2^2 \\ Q_3^2 + Q_1^3 \\ Q_4^2 + Q_2^3 \\ Q_3^3 \\ Q_4^3 \end{Bmatrix}$$

The boundary conditions and equilibrium of internal forces and moments are given by

$$Q_2^1 = 0, \quad Q_3^1 + Q_1^2 = 0, \quad Q_4^1 + Q_2^2 = 0, \quad Q_3^2 + Q_1^3 = F_0, \quad Q_4^2 + Q_2^3 = -aF_0$$

Note that the forces  $Q_1^1$  and  $Q_3^3$  and the moment  $Q_4^3$  (the reactions at the supports) are not known. The boundary conditions on the generalized displacements are

$$\left[ EI \frac{d^3 w}{dx^3} + kw \right]_{x=0} = 0 \Rightarrow Q_1^1 + kU_1 = 0; \quad w(28) = 0 \Rightarrow U_7 = 0; \quad \left( \frac{dw}{dx} \right) \Big|_{x=28} = 0 \Rightarrow U_8 = 0$$

Using the boundary and equilibrium conditions listed above, we can write the condensed equations for the unknown generalized displacements and forces. The condensed equations for the unknown generalized displacements can be obtained by deleting the last two rows and two columns, which correspond to the known  $U_i$  ( $F_0 = 10^3$  lb):

$$10^7 \begin{bmatrix} 0.24 + \alpha & -1.200 & -0.240 & -1.200 & 0.000 & 0.000 \\ & 8.000 & 1.200 & 4.000 & 0.000 & 0.000 \\ & & 0.309 & 0.783 & -0.069 & -0.417 \\ & & & 11.333 & 0.417 & 1.667 \\ & & \text{symmetric} & & 0.625 & -1.250 \\ & & & & & 10.000 \end{bmatrix} \begin{Bmatrix} U_1 \\ U_2 \\ U_3 \\ U_4 \\ U_5 \\ U_6 \end{Bmatrix} = 10^3 \begin{Bmatrix} 12 \\ -20 \\ 12 \\ 20 \\ 10 \\ -10 \end{Bmatrix}$$

where  $\alpha = 10^{-7}k$ . The unknown reactions can be computed from ( $Q_1^1 = -kU_1$ )

$$\begin{Bmatrix} Q_3^3 \\ Q_4^3 \end{Bmatrix} = 10^7 \begin{bmatrix} -0.5556 & 1.6667 \\ -1.6667 & 3.3333 \end{bmatrix} \begin{Bmatrix} U_5 \\ U_6 \end{Bmatrix}$$

This completes the finite element analysis of the problem.

The solution (with the help of a computer) of the condensed equations for the generalized displacements, when  $k = 10^{11}$  lb/in. (a hard spring), gives  $U_1 = 0.18356 \times 10^{-6} \approx 0$ , and (rounded to six decimal points)

$$U_2 = -0.003686, \quad U_3 = 0.026560 \text{ ft.}, \quad U_4 = -0.001097, \quad U_5 = 0.010215 \text{ ft.}, \quad U_6 = 0.002466$$

The reaction forces, from the element equilibrium equations, are

$$(Q_1^1)_{\text{equil}} = -kU_1 = -18,356 \text{ lb}, \quad (Q_3^3)_{\text{equil}} = -15,644 \text{ lb}, \quad (Q_4^3)_{\text{equil}} = -88,040 \text{ ft-lb}$$

Based on the definitions, we have

$$(Q_3^3)_{\text{def}} = -15,644 \text{ lb}, \quad (Q_4^3)_{\text{def}} = -88,038 \text{ ft-lb}$$

For  $k = 10^5$  lb/in. (a soft spring or no spring), we obtain

$$U_1 = 0.16104 \text{ ft.}, \quad U_2 = 0.004579, \quad U_3 = 0.10682 \text{ ft.}, \quad U_4 = 0.006605$$

$$U_5 = 0.020755 \text{ ft.}, \quad U_6 = 0.005844$$

Because of the discontinuity in the loading and the flexural rigidity, the exact solution  $w(x)$  is also defined by three separate expressions for the three regions.

### Example 5.2.3

This example deals with the indeterminate beam shown in Fig. 5.2.12. The beam is made of steel ( $E = 30 \times 10^6$  psi) and the cross-sectional dimensions are  $2 \times 3$  in. ( $I = 4.5 \text{ in.}^4$ ). We are interested in finding the transverse deflection  $w$  using the Euler-Bernoulli beam finite element.

Because of the discontinuity in loading, the beam should be divided into three elements:  $\Omega_1 = (0, 16)$ ,  $\Omega_2 = (16, 36)$ , and  $\Omega_3 = (36, 48)$ ; the element lengths are:  $h_1 = 16$  in.,  $h_2 = 20$  in., and  $h_3 = 12$  in. The load variation in each element is given by

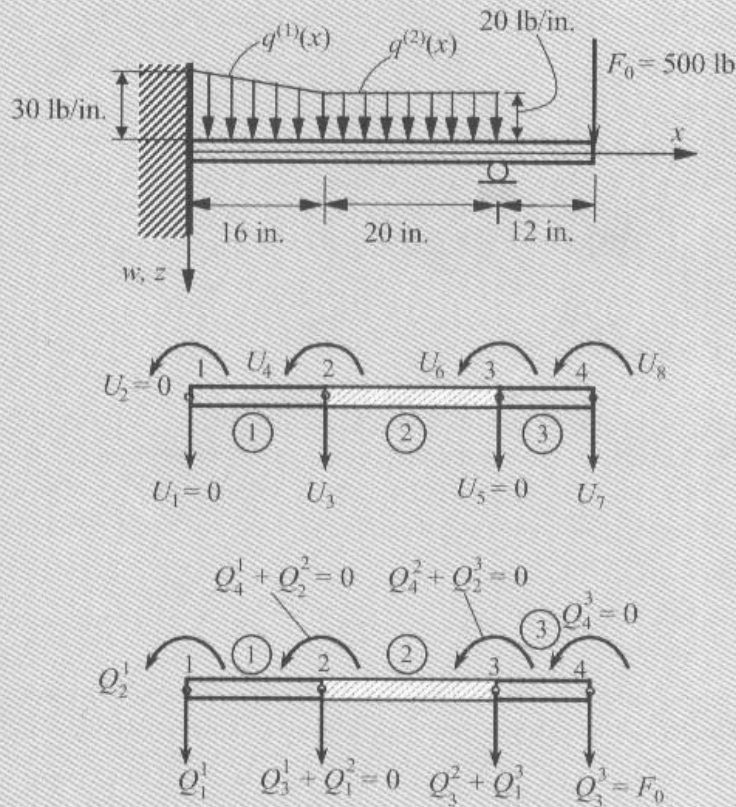
$$q^{(1)}(x) = \left(30 - \frac{10}{16}x\right), \quad q^{(2)}(x) = 20, \quad q^{(3)}(x) = 0$$

Using Eq. (5.2.19), we obtain the following load vectors due to the distributed loads:

$$\{q^1\} = \begin{Bmatrix} 216.00 \\ -554.67 \\ 184.00 \\ 512.00 \end{Bmatrix}, \quad \{q^2\} = \begin{Bmatrix} 200.00 \\ -666.77 \\ 200.00 \\ 666.67 \end{Bmatrix}, \quad \{q^3\} = \{0\}$$

The element stiffness matrices can be computed from Eq. (5.2.18) by substituting appropriate values of  $h$ ,  $E$ ,  $I$ , and  $c_f = 0$ . For Element 1, for example, we have ( $h_1 = 16$  in.,  $EI = 135 \times 10^6$  lb-in.<sup>2</sup>),

$$[K^1] = 10^6 \begin{bmatrix} 0.3955 & -3.1641 & -0.3955 & -3.1641 \\ -3.1641 & 33.7500 & 3.1641 & 16.8750 \\ -0.3955 & 3.1641 & 0.3955 & 3.1641 \\ -3.1641 & 16.8750 & 3.1641 & 33.7500 \end{bmatrix}$$



**Figure 5.2.12** Finite element modeling of an indeterminate beam.

The assembled stiffness matrix and load vector for this mesh is of the same form as given in Eqs. (5.2.24a) and (5.2.24b). The boundary conditions for the problem are

$$w(0) = 0 \rightarrow U_1 = 0, \quad \frac{dw}{dx}(0) = 0 \rightarrow U_2 = 0, \quad w(36) = 0 \rightarrow U_5 = 0$$

$$Q_3^1 + Q_3^2 = 0, \quad Q_4^1 + Q_4^2 = 0, \quad Q_4^2 + Q_4^3 = 0, \quad Q_3^3 = 500, \quad Q_4^3 = 0$$

Note that  $Q_1^1$ ,  $Q_2^1$ , and  $Q_3^1 + Q_3^2$  are the reactions that are not known and are to be calculated in the postcomputation. Since the specified boundary conditions on the primary variables are homogeneous, we can delete the rows and columns corresponding to the specified displacements (i.e., delete rows and columns 1, 2, and 5) and solve the remaining five equations for  $U_3$ ,  $U_4$ ,  $U_6$ ,  $U_7$ , and  $U_8$ :

$$U_3 = -0.000322 \text{ in.}, \quad U_4 = 0.0000593 \text{ rad.}, \quad U_6 = -0.0002513 \text{ rad.}$$

$$U_7 = 0.00515 \text{ in.}, \quad U_8 = -0.000518 \text{ rad.}$$

The exact deflection in the three intervals of the beam is given by (large numbers were rounded to whole numbers)

$$w(x) = \begin{cases} \frac{1}{EI} \left( 268.543x^2 - \frac{691}{15}x^3 + \frac{5}{4}x^4 - \frac{1}{192}x^5 \right) & 0 \leq x \leq 16 \\ \frac{1}{EI} \left( -\frac{16,384}{3} + \frac{5120}{3}x + 55.2097x^2 - \frac{491}{15}x^3 + \frac{5}{6}x^4 \right) & 16 \leq x \leq 36 \\ \frac{1}{EI} \left( 6,554,368 - 506,066x + 12,000x^2 - \frac{250}{3}x^3 \right) & 36 \leq x \leq 48 \end{cases}$$

A comparison of the finite element solutions for deflections ( $w$ ), slopes ( $\theta$ ), and bending moments ( $M$ ) (calculated in the postcomputation) at points other than the nodes are compared with the exact values in Table 5.2.3 for three different meshes. The values of deflections, slopes, and bending moments were computed using the finite element solution and its derivatives.

**Table 5.2.3** Comparison of the finite element solution with the exact solution (units of the quantities should be obvious) of the beam problem considered in Example 5.2.3.

$x$	$N^\dagger$	$w_0 \times 10^6$		$(-dw_0/dx) \times 10^6$		$-(d^2w_0/dx^2) \times 10^6$	
		FEM	Exact	FEM	Exact	FEM	Exact
2.0	3	-0.8570		1.1553		-1.0250	
	5	4.1405	5.3739	-3.3386	-4.1552	0.4663	0.3219
	6	5.2319		-4.1558		0.4638	
6.0	3	-18.4510		8.8348		-2.8147	
	5	8.3936	9.6048	4.4199	5.2328	-4.3456	-4.4727
	6	9.4751		5.2323		-4.3431	
12.0	3	-138.2300		33.7760		-5.4992	
	5	-122.5900	-120.8100	39.6630	39.6720	-5.4794	-5.9238
	6	-122.5900		39.6630		-5.4794	
21.0	3	-674.3600		71.5620		3.5507	
	5	-643.4900	-639.6300	62.3030	62.3020	3.5507	2.9335
	6	-643.4900		62.3030		3.5507	
31.0	3	-812.9300		-83.7970		27.5210	
	5	-782.0700	-778.1900	-74.5370	-74.5390	27.5210	26.9040
	6	-782.0700		-74.5370		27.5210	
42.0	3	2174.9000		-451.3600		22.2220	
	5	2174.9000	2174.8000	-451.3600	-451.3600	22.2220	22.2220
	6	2174.9000		-451.3600		22.2220	

<sup>†</sup>3-Elements:  $h_1 = 16, h_2 = 20, h_3 = 12$ . 5-Elements:  $h_1 = 8, h_2 = 8, h_3 = 10, h_4 = 10, h_5 = 12$ . 6-Elements:  $h_1 = 4, h_2 = 4, h_3 = 8, h_4 = 10, h_5 = 10, h_6 = 12$ .

**Example 5.2.4** (Beam Element with Nodal Hinge)

The last example of this section deals with a beam with an internal hinge (see Fig. 5.2.13). It is not uncommon to find beams with an internal hinge about which the beam is free to rotate. Thus, at the hinge there cannot be any moment and the rotation is *not* continuous across the hinge. To account for the discontinuity in the rotation at a hinge, we must eliminate the rotation associated with the hinge.

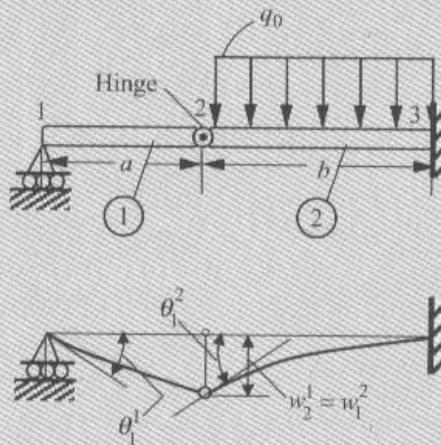
Consider a uniform beam element with a hinge at node 2. The element equation is given by Eq. (5.2.17) with the stiffness matrix given in (5.2.18) (with zero foundation modulus,  $c_f = 0$ )

$$\frac{2EI}{h^3} \begin{bmatrix} 6 & -3h & -6 & \vdots & -3h \\ -3h & 2h^2 & 3h & \vdots & h^2 \\ -6 & 3h & 6 & \vdots & 3h \\ \dots & \dots & \dots & \vdots & \dots \\ -3h & h^2 & 3h & \vdots & 2h^2 \end{bmatrix} \begin{Bmatrix} w_1 \\ \theta_1 \\ w_2 \\ \dots \\ \theta_2 \end{Bmatrix} = \begin{Bmatrix} F_1 \\ F_2 \\ F_3 \\ \dots \\ F_4 \end{Bmatrix} \quad (5.2.35)$$

Since the moment at a hinge is zero, we have  $Q_4 = 0$  and  $F_4 = q_4 + Q_4 = q_4$ , which is known. This allows us to eliminate  $\theta_2$  (rotation at node 2) using the method discussed in Eqs. (3.2.59)–(3.2.60). Comparing Eq. (5.2.35) with Eq. (3.2.59), we have the following definitions:

$$\mathbf{K}^{11} = \frac{2EI}{h^3} \begin{bmatrix} 6 & -3h & -6 \\ -3h & 2h^2 & 3h \\ -6 & 3h & 6 \end{bmatrix}, \quad \mathbf{K}^{12} = \frac{2EI}{h^3} \begin{Bmatrix} -3h \\ h^2 \\ 3h \end{Bmatrix}, \quad \mathbf{K}^{21} = (\mathbf{K}^{12})^T$$

$$\mathbf{K}^{22} = \frac{4EI}{h}, \quad \mathbf{U}^1 = \begin{Bmatrix} w_1 \\ \theta_1 \\ w_2 \end{Bmatrix}, \quad \mathbf{U}^2 = \theta_2$$



**Figure 5.2.13** Compound beam with an internal hinge.

Substituting (3.2.60c) for  $U^2 = \theta_2$  into (3.2.60a), we obtain

$$\begin{aligned}\hat{\mathbf{K}} &= \mathbf{K}^{11} - \mathbf{K}^{12} (\mathbf{K}^{22})^{-1} \mathbf{K}^{21} \\ &= \frac{EI}{h^3} \begin{bmatrix} 12 & -6h & -12 \\ -6h & 4h^2 & 6h \\ -12 & 6h & 12 \end{bmatrix} - \frac{2EI}{h^3} \begin{bmatrix} -3h \\ h^2 \\ 3h \end{bmatrix} \frac{h}{4EI} \frac{2EI}{h^3} \{-3h \ h^2 \ 3h\} \\ &= \frac{3EI}{h^3} \begin{bmatrix} 1 & -h & -1 \\ -h & h^2 & h \\ -1 & h & 1 \end{bmatrix}\end{aligned}$$

Thus, the equations for a beam element with a hinge at node 2 can be written as

$$\frac{3EI}{h^3} \begin{bmatrix} 1 & -h & -1 & 0 \\ -h & h^2 & h & 0 \\ -1 & h & 1 & 0 \\ 0 & 0 & 0 & 0 \end{bmatrix} \begin{Bmatrix} w_1 \\ \theta_1 \\ w_2 \\ \theta_2 \end{Bmatrix} = \begin{Bmatrix} F_1 \\ F_2 \\ F_3 \\ 0 \end{Bmatrix} \quad (5.2.36)$$

Similarly, we can derive the element equations for a beam element with hinge at node 1

$$\frac{3EI}{h^3} \begin{bmatrix} 1 & 0 & -1 & -h \\ 0 & 0 & 0 & 0 \\ -1 & 0 & 1 & h \\ -h & 0 & h & h^2 \end{bmatrix} \begin{Bmatrix} w_1 \\ \theta_1 \\ w_2 \\ \theta_2 \end{Bmatrix} = \begin{Bmatrix} F_1 \\ 0 \\ F_3 \\ F_4 \end{Bmatrix} \quad (5.2.37)$$

As a specific example of application of the equations derived, consider the beam in Fig. 5.2.13. We use a two-element mesh, with element 1 having the hinge at its node 2, while element 2 is the usual beam element. The assembled system of equations is

$$EI \begin{bmatrix} \frac{3}{a^3} & -\frac{3}{a^2} & -\frac{3}{a^2} & 0 & 0 & 0 \\ -\frac{3}{a^3} & \frac{3}{a^2} & \frac{3}{a^2} & 0 & 0 & 0 \\ -\frac{3}{a^3} & \frac{3}{a^2} & \frac{3}{a^2} + \frac{12}{b^3} & -\frac{6}{b^2} & -\frac{12}{b^3} & -\frac{6}{b^2} \\ 0 & 0 & -\frac{6}{b^2} & \frac{4}{b} & \frac{6}{b^2} & \frac{2}{b} \\ 0 & 0 & -\frac{12}{b^3} & \frac{6}{b^2} & \frac{12}{b^3} & \frac{6}{b^2} \\ 0 & 0 & -\frac{6}{b^2} & \frac{2}{b} & \frac{6}{b^2} & \frac{4}{b} \end{bmatrix} \begin{Bmatrix} w_1^1 \\ \theta_1^1 \\ w_2^1 = w_1^2 \\ \theta_1^2 \\ w_2^2 \\ \theta_2^2 \end{Bmatrix} = \begin{Bmatrix} Q_1^1 \\ Q_2^1 \\ Q_3^1 + Q_4^2 \\ Q_4^1 + Q_2^2 \\ Q_3^2 \\ Q_4^2 \end{Bmatrix} + \frac{q_0 b}{12} \begin{Bmatrix} 0 \\ 0 \\ 6 \\ -b \\ 6 \\ b \end{Bmatrix} \quad (5.2.38)$$

Using the boundary conditions

$$w_1^1 = 0, \quad w_2^2 = 0, \quad \theta_2^2 = 0, \quad Q_2^1 = 0, \quad Q_3^1 + Q_4^2 = 0, \quad Q_4^1 + Q_2^2 = 0$$

we obtain the condensed equations

$$EI \begin{bmatrix} \frac{3}{a^3} & \frac{3}{a^2} & 0 \\ \frac{3}{a^3} & \frac{3}{a^2} + \frac{12}{b^3} & -\frac{6}{b^2} \\ 0 & -\frac{6}{b^2} & \frac{4}{b} \end{bmatrix} \begin{Bmatrix} \theta_1^1 \\ w_2^1 = w_1^2 \\ \theta_1^2 \end{Bmatrix} = \frac{q_0 b}{12} \begin{Bmatrix} 0 \\ 6 \\ -b \end{Bmatrix} \quad (5.2.39)$$

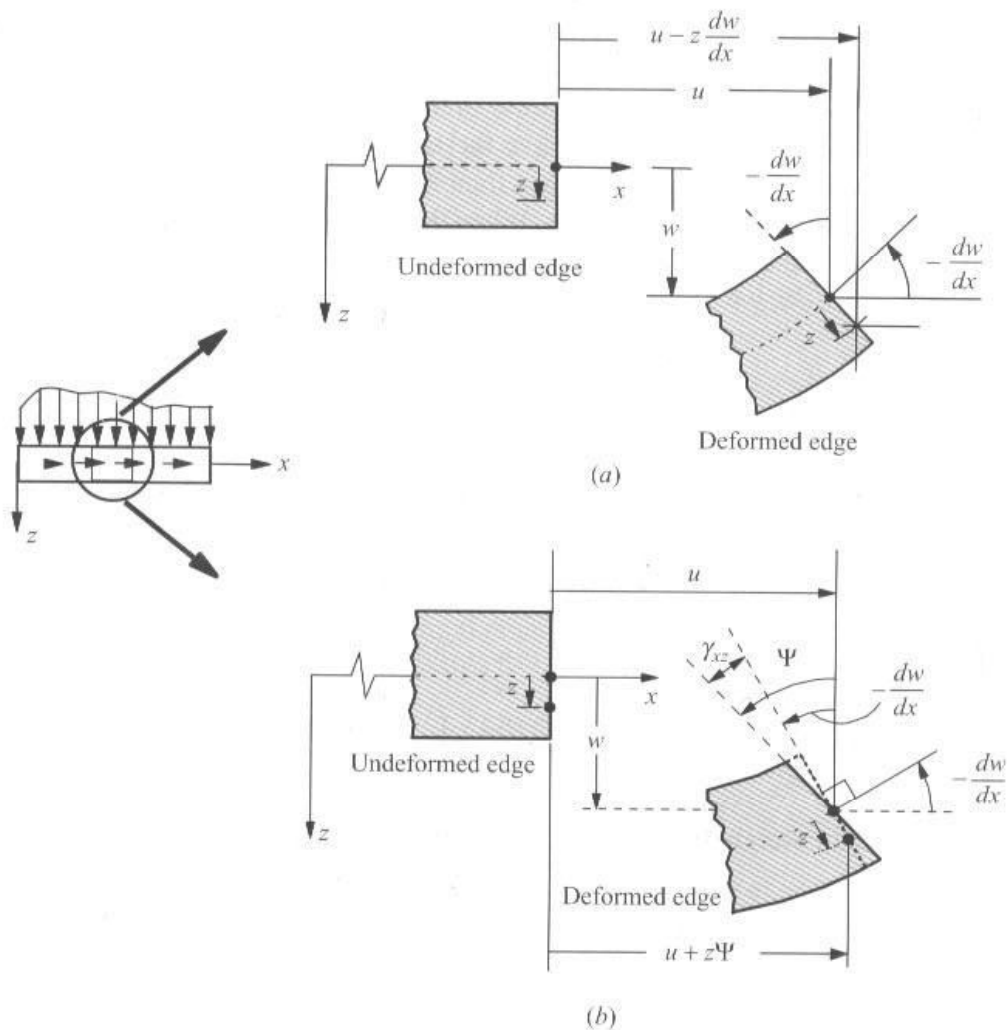
and the solution is given by

$$\theta_1^1 = -\frac{q_0 b^4}{8aEI}, \quad w_2^1 = w_1^2 = \frac{q_0 b^4}{8EI}, \quad \theta_2^2 = \frac{q_0 b^3}{2EI}$$

## 5.3 TIMOSHENKO BEAM ELEMENTS

### 5.3.1 Governing Equations

Recall that the Euler–Bernoulli beam theory is based on the assumption that plane cross sections remain plane and *normal* to the longitudinal axis after bending [see Fig. 5.3.1(a)]. This assumption results in zero transverse shear strain. When the normality assumption is not used, i.e., plane sections remain plane but not necessarily normal to the longitudinal axis after deformation, the transverse shear strain  $\gamma_{xz} = 2\varepsilon_{xz}$  is not zero. Therefore, the rotation



**Figure 5.3.1** (a) Kinematics of the Euler–Bernoulli beam theory. (b) Kinematics of the Timoshenko beam theory where normals before deformation no longer remain normal after deformation.

of a transverse normal plane about the  $y$ -axis is not equal to  $-dw/dx$  [see Fig. 5.3.1(b)]. Beam theory based on these relaxed assumptions is known as a *shear deformation beam theory*, most commonly known as the *Timoshenko beam theory*. We denote the rotation about the  $y$ -axis by an independent function  $\Psi(x)$ .

The equilibrium equations of the Timoshenko beam theory [see Example 2.4.3; also see Reddy (2002)] are the same as those of the Euler–Bernoulli beam theory (see Fig. 5.2.1), but the kinematic relations are different:

$$-\frac{dV}{dx} + c_f w = q, \quad -\frac{dM}{dx} + V = 0, \quad M = EI \frac{d\Psi}{dx}, \quad V = GAK_s \left( \frac{dw}{dx} + \Psi \right) \quad (5.3.1)$$

Thus, the governing equations in terms of the deflection  $w$  and rotation  $\Psi$  become

$$-\frac{d}{dx} \left[ GAK_s \left( \Psi + \frac{dw}{dx} \right) \right] + c_f w = q \quad (5.3.2a)$$

$$-\frac{d}{dx} \left( EI \frac{d\Psi}{dx} \right) + GAK_s \left( \Psi + \frac{dw}{dx} \right) = 0 \quad (5.3.2b)$$

where  $G$  is the shear modulus and  $K_s$  is the *shear correction coefficient*, which is introduced to account for the difference in the constant state of shear stress in this theory and the parabolic variation of the shear stress predicted by the elasticity theory through the beam thickness. All other quantities have the same meaning as before. For short and chubby beams (i.e., length-to-height ratio less than 20),  $\Psi \neq -(dw/dx)$  and the difference,  $\Psi + (dw/dx)$ , is the transverse shear strain. When the shear strain is zero (i.e., for long slender beams), substituting the second equation into the first for  $GAK_s(\Psi + dw/dx)$  and replacing  $\Psi$  with  $-dw/dx$ , we obtain governing equation (5.2.1) of the Euler–Bernoulli beam theory.

### 5.3.2 Weak Form

The weak form of Eqs. (5.3.2a) and (5.3.2b) over an element  $\Omega^e = (x_a, x_b)$  can be developed using the usual three-step procedure, as already discussed in Example 2.4.3. At the end of the second step (i.e., after integration by parts), we obtain

$$0 = \int_{x_a}^{x_b} \left[ \frac{dv_1}{dx} GAK_s \left( \Psi + \frac{dw}{dx} \right) + c_f v_1 w - v_1 q \right] dx - \left[ v_1 GAK_s \left( \Psi + \frac{dw}{dx} \right) \right]_{x_a}^{x_b}$$

$$0 = \int_{x_a}^{x_b} \left[ \frac{dv_2}{dx} EI \frac{d\Psi}{dx} + v_2 GAK_s \left( \Psi + \frac{dw}{dx} \right) \right] dx - \left[ v_2 EI \frac{d\Psi}{dx} \right]_{x_a}^{x_b}$$

The coefficients of the weight functions  $v_1$  and  $v_2$  in the boundary integrals are, respectively,

$$GAK_s \left( \Psi + \frac{dw}{dx} \right) \equiv V \quad \text{and} \quad EI \frac{d\Psi}{dx} \equiv M \quad (5.3.3)$$

where  $V$  is the shear force and  $M$  is the bending moment; these coefficients constitute the secondary variables of the weak form. The weight functions  $v_1$  and  $v_2$  must have the physical interpretations such that the products  $v_1 V$  and  $v_2 M$  have the units of work. Clearly,  $v_1$  must be equivalent to (the variation of) the transverse deflection  $w$ , and  $v_2$  must be equivalent to

(the variation of) the rotation function  $\Psi$ :

$$v_1 \sim w, \quad v_2 \sim \Psi$$

Hence, the primary variable of the formulation are  $w$  and  $\Psi$ . Denoting the shear forces and bending moments at the endpoints of the element by the expressions [cf. Eq. (5.2.3)]

$$\begin{aligned} Q_1^e &\equiv - \left[ GAK_s \left( \Psi + \frac{dw}{dx} \right) \right] \Big|_{x_a} = -V(x_a) \\ Q_2^e &\equiv - \left( EI \frac{d\Psi}{dx} \right) \Big|_{x_a} = -M(x_a) \\ Q_3^e &\equiv \left[ GAK_s \left( \Psi + \frac{dw}{dx} \right) \right] \Big|_{x_b} = V(x_b) \\ Q_4^e &\equiv \left( EI \frac{d\Psi}{dx} \right) \Big|_{x_b} = M(x_b) \end{aligned} \quad (5.3.4)$$

we arrive at the final weak statements of Eqs. (5.3.2a) and (5.3.2b):

$$\begin{aligned} 0 &= \int_{x_a}^{x_b} \left[ GAK_s \frac{dv_1}{dx} \left( \Psi + \frac{dw}{dx} \right) + c_f v_1 w - v_1 q \right] dx - v_1(x_a) Q_1^e - v_1(x_b) Q_3^e \\ 0 &= \int_{x_a}^{x_b} \left[ EI \frac{dv_2}{dx} \frac{d\Psi}{dx} + GAK_s v_2 \left( \Psi + \frac{dw}{dx} \right) \right] dx - v_2(x_a) Q_2^e - v_2(x_b) Q_4^e \end{aligned} \quad (5.3.5)$$

We note that  $Q_i^e$  have the same meaning as well as sense as in the Euler–Bernoulli beam theory.

We can identify the bilinear and linear forms from the weak forms as

$$\begin{aligned} B((v_1, v_2), (w, \Psi)) &= \int_{x_a}^{x_b} \left[ GAK_s \left( \frac{dv_1}{dx} + v_2 \right) \left( \Psi + \frac{dw}{dx} \right) + EI \frac{dv_2}{dx} \frac{d\Psi}{dx} \right] dx \\ l((v_1, v_2)) &= \int_{x_a}^{x_b} v_1 q dx + v_1(x_a) Q_1^e + v_2(x_a) Q_2^e + v_1(x_b) Q_3^e + v_2(x_b) Q_4^e \end{aligned} \quad (5.3.6)$$

Equations (5.3.5) are equivalent to the statement of the principle of virtual displacements for the Timoshenko beam theory. The total potential energy functional of the isolated beam finite element is given by [see Eq. (2.4.40)]

$$\begin{aligned} \Pi_e(w, \Psi) &= \int_{x_e}^{x_{e+1}} \left[ \frac{EI}{2} \left( \frac{d\Psi}{dx} \right)^2 + \frac{GAK_s}{2} \left( \frac{dw}{dx} + \Psi \right)^2 + \frac{1}{2} c_f w^2 - wq \right] dx \\ &\quad - w(x_a) Q_1^e - \Psi(x_a) Q_2^e - w(x_b) Q_3^e - \Psi(x_b) Q_4^e \end{aligned} \quad (5.3.7)$$

The first term in the square brackets represents the elastic strain energy due to bending, the second term represents the elastic energy due to the transverse shear deformation, the third is the strain energy stored in the elastic foundation, and the fourth is the work done by the distributed load; the remaining terms account for the work done by the generalized forces  $Q_i^e$  in moving through the respective generalized displacements  $(w, \Psi)$  at the ends of the element. Once again, the principle of minimum total potential energy,  $\delta \Pi_e = 0$ , gives the weak forms in Eq. (5.3.5).

### 5.3.3 General Finite Element Model

A close examination of the terms in (5.3.5) shows that both  $w$  and  $\Psi$  are differentiated only once with respect to  $x$ . Since the primary variables are the dependent unknowns themselves (and do not include their derivatives), the Lagrange interpolation of both  $w$  and  $\Psi$  is admissible here. The minimum admissible degree of interpolation is linear, so that  $dw/dx \neq 0$  and  $d\Psi/dx \neq 0$ . The variables  $w$  and  $\Psi$  do not have the same physical units; they can be interpolated, in general, with different degrees of interpolation.

Let us consider Lagrange interpolation of  $w$  and  $\Psi$  in the form

$$w = \sum_{j=1}^m w_j \psi_j^{(1)}, \quad \Psi = \sum_{j=1}^n S_j \psi_j^{(2)} \quad (5.3.8)$$

where  $\psi_j^{(1)}$  and  $\psi_j^{(2)}$  are the Lagrange interpolation functions of degree  $m-1$  and  $n-1$ , respectively. In general,  $m$  and  $n$  are independent of each other, although  $m=n$  is most common. However, when  $m=n=2$  (i.e., linear interpolation of both  $w$  and  $\Psi$  is used; see Fig. 5.3.2), the derivative of  $w$  is

$$\left(\frac{dw}{dx}\right)^e = \frac{w_2^e - w_1^e}{h_e}$$

which is elementwise-constant. The rotation  $\Psi$ , being linear, is not consistent with that predicted by  $w(x)$ . For thin beams, the transverse shear deformation is negligible, and we must have  $\Psi = -dw/dx$ , which requires

$$S_1^e \frac{x_b - x}{h_e} + S_2^e \frac{x - x_a}{h_e} = -\frac{w_2^e - w_1^e}{h_e}$$

or, equivalently (by equating like coefficients on both sides),

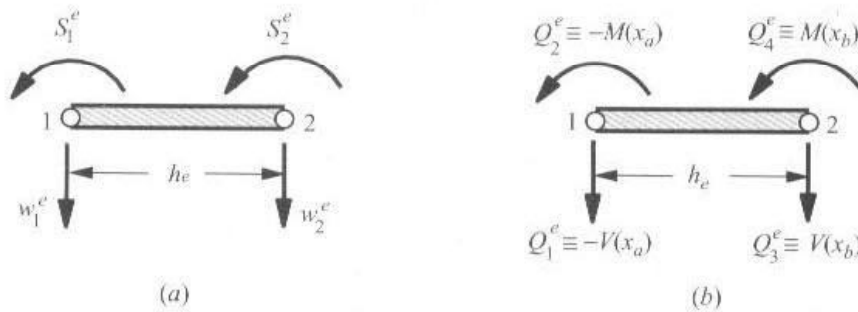
$$S_1^e x_b - S_2^e x_a = -(w_2^e - w_1^e), \quad S_2^e - S_1^e = 0$$

which in turn requires

$$S_1^e = S_2^e = -\frac{w_2^e - w_1^e}{h_e} \quad (5.3.9)$$

This implies that  $\Psi(x)$  is a constant, i.e.,  $S_1^e = S_2^e = S^e$ :

$$\Psi(x) = S_1^e \frac{x_b - x}{h_e} + S_2^e \frac{x - x_a}{h_e} = S^e \quad (5.3.10)$$



**Figure 5.3.2** Linear Timoshenko beam finite element. (a) Generalized displacements. (b) Generalized forces.

However, a constant state of  $\Psi(x)$  is not admissible because the bending energy of the element,

$$\int_{x_a}^{x_b} \frac{EI}{2} \left( \frac{d\Psi}{dx} \right)^2 dx \quad (5.3.11)$$

would be zero. This numerical problem is known in the finite element literature as *shear locking*.

To overcome shear locking, two alternative procedures have been used in the literature:

1. *Consistent interpolation*. Use an approximation of  $w$  and  $\Psi$  such that  $dw/dx$  and  $\Psi$  are polynomials of the same degree (i.e.,  $m = n + 1$ ).
2. *Reduced integration*. Use equal interpolation (i.e.,  $m = n$ ) for  $w$  and  $\Psi$  and evaluate the bending stiffness coefficients associated with (5.3.11) using a numerical integration rule (to be discussed in Chapter 7) consistent with the actual interpolation of  $\Psi$ . However, the stiffness coefficients associated with the shear energy

$$\int_{x_a}^{x_b} \frac{GAK_s}{2} \left( \frac{dw}{dx} + \Psi \right)^2 dx \quad (5.3.12)$$

must be evaluated using a numerical integration rule that treats  $\Psi$  as if it is the same order polynomial as  $dw/dx$ . Thus, if  $w$  and  $\Psi$  are approximated with linear polynomials,  $dw/dx$  is a constant and  $\Psi$  is linear. In evaluating the stiffness terms coming from the shear energy (5.3.12), we must use one-point integration, as dictated by  $dw/dx$  and not  $\Psi$ . Note that one-point integration in this case is sufficient to evaluate the bending energy exactly but not the shear energy because it is quadratic in  $\Psi$ . Thus, it amounts to underintegrating the term. This is known as the *reduced integration* technique.

For illustrative purposes, we take a detailed look at the expression

$$\frac{GAK_s}{2} \int_{x_a}^{x_b} \left( \frac{dw}{dx} + \Psi \right)^2 dx = \frac{GAK_s}{2} \left[ \left( \frac{dw}{dx} + \Psi \right)^2 \Big|_{x=x_a+h_e/2} \right] h_e$$

where  $x = x_a + \frac{1}{2}h_e$  is the midpoint of the element and  $h_e$  is its length. Substituting (5.3.8) into this expression (with  $m = n = 2$ ) and equating to zero for thin beams, we obtain

$$\begin{aligned} & \frac{GAK_s h_e}{2} \left( \frac{w_2^e - w_1^e}{h_e} + S_1^e \frac{x_b - x}{h_e} + S_2^e \frac{x - x_a}{h_e} \right)^2 \Big|_{x=x_a+h_e/2} \\ &= \frac{GAK_s h_e}{2} \left( \frac{w_2^e - w_1^e}{h_e} + \frac{S_1^e + S_2^e}{2} \right)^2 = 0 \end{aligned} \quad (5.3.13)$$

which is a weaker requirement than (5.3.9), i.e., if (5.3.9) holds, then (5.3.13) also holds, but (5.3.13) does not imply (5.3.9). We note that (5.3.9) must hold only for problems for which the transverse shear energy (5.3.12) is negligible.

In summary, we use either consistent interpolation ( $m = n + 1$ ) or equal interpolation with reduced integration in the evaluation of the transverse shear stiffness coefficients in the Timoshenko beam element. We consider both forms of elements here. First, we complete the finite element model development using the general interpolations given in Eq. (5.3.8) and then discuss the specific choice of interpolations functions used for  $w$  and  $\Psi$ .

Substitution of (5.3.8) for  $w$  and  $\Psi$ , and  $v_1 = \psi_i^{(1)}$  and  $v_2 = \psi_i^{(2)}$  into the weak forms (5.3.5), we obtain the following finite element equations of the Timoshenko beam element:

$$\begin{aligned} 0 &= \sum_{j=1}^m K_{ij}^{11} w_j + \sum_{j=1}^n K_{ij}^{12} s_j - F_i^1 \quad (i = 1, 2, \dots, m) \\ 0 &= \sum_{j=1}^m K_{ij}^{21} w_j + \sum_{j=1}^n K_{ij}^{22} s_j - F_i^2 \quad (i = 1, 2, \dots, n) \end{aligned} \quad (5.3.14)$$

where

$$\begin{aligned} K_{ij}^{11} &= \int_{x_a}^{x_b} \left( GAK_s \frac{d\psi_i^{(1)}}{dx} \frac{d\psi_j^{(1)}}{dx} + c_f \psi_i^{(1)} \psi_j^{(1)} \right) dx \\ K_{ij}^{12} &= \int_{x_a}^{x_b} GAK_s \frac{d\psi_i^{(1)}}{dx} \psi_j^{(2)} dx = K_{ji}^{21} \quad (\text{i.e., } [K^{21}] = [K^{12}]^T) \\ K_{ij}^{22} &= \int_{x_a}^{x_b} \left( EI \frac{d\psi_i^{(2)}}{dx} \frac{d\psi_j^{(2)}}{dx} + GAK_s \psi_i^{(2)} \psi_j^{(2)} \right) dx \\ F_i^1 &= \int_{x_a}^{x_b} q \psi_i^{(1)} dx + Q_{2i-1}, \quad F_i^2 = Q_{2i} \end{aligned} \quad (5.3.15)$$

In the interest of clarity, the element label  $e$  on the quantities is omitted. Equations (5.3.14) can be written in matrix form as

$$\begin{bmatrix} [K^{11}] & [K^{12}] \\ [K^{21}] & [K^{22}] \end{bmatrix} \begin{Bmatrix} \{w\} \\ \{s\} \end{Bmatrix} = \begin{Bmatrix} \{F^1\} \\ \{F^2\} \end{Bmatrix} \quad (5.3.16)$$

The finite element model in (5.3.16) with the coefficients given in (5.3.15) is the most general displacement finite element model of the Timoshenko beam theory. It can be used to obtain a number of special finite element models, as discussed next.

### 5.3.4 Consistent Interpolation Elements

The first consistent interpolation element (CIE) that we will consider is the one in which quadratic interpolation is used for  $w$  and linear interpolation for  $\Psi$  so that  $dw/dx$  and  $\Psi$  are of the same order polynomial (and hence, no shear locking occurs). That is, we select  $\psi_i^{(1)}$  to be quadratic polynomials and  $\psi_i^{(2)}$  to be linear polynomials. For this choice of interpolation,  $[K^{11}]$  is  $3 \times 3$ ,  $[K^{12}]$  is  $3 \times 2$ , and  $[K^{22}]$  is  $2 \times 2$ . The explicit forms of the matrices, when  $EI$  and  $GAK_s$  are constant, are (note that some of the matrix coefficients are readily available from Chapter 3)

$$[K^{11}] = \frac{G_e A_e K_s}{3h_e} \begin{bmatrix} 7 & -8 & 1 \\ -8 & 16 & -8 \\ 1 & -8 & 7 \end{bmatrix} + \frac{c_f^e h_e}{30} \begin{bmatrix} 4 & 2 & -1 \\ 2 & 16 & 2 \\ -1 & 2 & 4 \end{bmatrix}$$

$$[K^{12}] = \frac{G_e A_e K_s}{6} \begin{bmatrix} -5 & -1 \\ 4 & -4 \\ 1 & 5 \end{bmatrix} = [K^{21}]^T$$

$$[K^{22}] = \frac{EI}{h_e} \begin{bmatrix} 1 & -1 \\ -1 & 1 \end{bmatrix} + \frac{G_e A_e K_s h_e}{6} \begin{bmatrix} 2 & 1 \\ 1 & 2 \end{bmatrix} \quad (5.3.17)$$

When  $c_f = 0$ , the finite element equations for this choice of interpolation are given by (see Fig. 5.3.3)

$$\frac{G A K_s}{6 h_e} \begin{bmatrix} 14 & -16 & 2 & -5h_e & -h_e \\ -16 & 32 & -16 & 4h_e & -4h_e \\ 2 & -16 & 14 & h_e & 5h_e \\ -5h_e & 4h_e & h_e & 2h_e^2 \Sigma_e & h_e^2 \Theta_e \\ -h_e & -4h_e & 5h_e & h_e^2 \Theta_e & 2h_e^2 \Sigma_e \end{bmatrix} \begin{Bmatrix} w_1^e \\ w_c^e \\ w_2^e \\ S_1^e \\ S_2^e \end{Bmatrix} = \begin{Bmatrix} q_1^e \\ q_c^e \\ q_2^e \\ 0 \\ 0 \end{Bmatrix} + \begin{Bmatrix} Q_1^e \\ \hat{Q}_c^e \\ Q_3^e \\ Q_2^e \\ Q_4^e \end{Bmatrix} \quad (5.3.18)$$

where

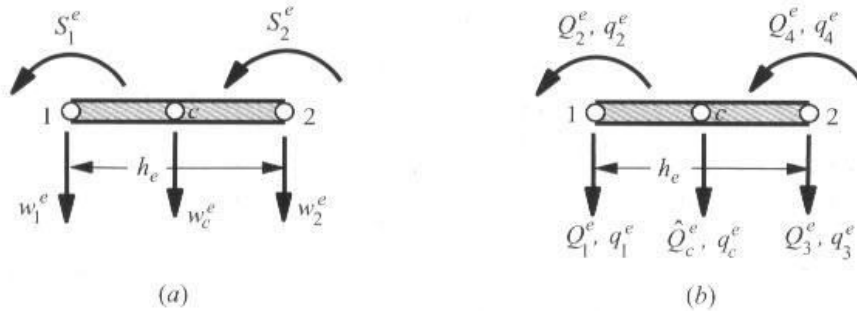
$$\Lambda_e = \frac{E_e I_e}{G_e A_e K_s h_e^2}, \quad \mu_0 = 12\Lambda_e, \quad \Theta_e = 1 - 6\Lambda_e, \quad \Sigma_e = 1 + 3\Lambda_e \quad (5.3.19)$$

$(Q_1^e, Q_2^e, Q_3^e, Q_4^e)$  are the generalized forces defined in Eq. (5.3.4),  $w_c^e$  and  $\hat{Q}_c^e$  are the deflection and applied external load, respectively, at the center node of the quadratic element, and

$$q_i^e = \int_{x_a}^{x_b} \psi_i^{(1)} q \, dx, \quad (i = 1, 2, c), \quad \psi_i^{(1)} = \text{quadratic} \quad (5.3.20)$$

This element is designated as CIE-1 (see Fig. 5.3.3).

Note that node  $c$ , which is the center node of the element, is not connected to other elements, and the only degree of freedom there is the transverse deflection. Thus, there are different number of degrees of freedom at different nodes of the element, and this therefore complicates the assembly of elements and its implementation on a computer. Hence, we eliminate the node  $c$  dependence in the system of element equations by condensing out  $w_c^e$ . The second equation of (5.3.18) can be used to express  $w_c^e$  in terms of  $w_1^e, w_2^e, S_1^e, S_2^e, q_c^e$ ,



**Figure 5.3.3** Consistent interpolation Timoshenko beam element, CIE-1. (a) Generalized displacements. (b) Generalized forces.

and  $\hat{Q}_c^e$ :

$$w_c^e = \frac{6h_e}{32G_e A_e K_s} (q_c^e + \hat{Q}_c^e) + \left( \frac{w_1^e + w_2^e}{2} \right) + h_e \left( \frac{S_2^e - S_1^e}{8} \right) \quad (5.3.21)$$

Substituting for  $w_c^e$  from Eq. (5.3.21) into the remaining equations of (5.3.18) [i.e., eliminate  $w_c^e$  from Eq. (5.3.18)] and rearranging the equations, we obtain

$$\begin{aligned} \left( \frac{2E_e I_e}{\mu_0 h_e^3} \right) \begin{bmatrix} 6 & -3h_e & -6 & -3h_e \\ -3h_e & h_e^2(1.5 + 6\Lambda_e) & 3h_e & h_e^2(1.5 - 6\Lambda_e) \\ -6 & 3h_e & 6 & 3h_e \\ -3h_e & h_e^2(1.5 - 6\Lambda_e) & 3h_e & h_e^2(1.5 + 6\Lambda_e) \end{bmatrix} \begin{Bmatrix} w_1^e \\ S_1^e \\ w_2^e \\ S_2^e \end{Bmatrix} \\ = \begin{Bmatrix} q_1^e + \frac{1}{2}\hat{q}_c^e \\ -\frac{1}{8}\hat{q}_c^e h_e \\ q_2^e + \frac{1}{2}\hat{q}_c^e \\ \frac{1}{8}\hat{q}_c^e h_e \end{Bmatrix} + \begin{Bmatrix} Q_1^e \\ Q_2^e \\ Q_3^e \\ Q_4^e \end{Bmatrix} \end{aligned} \quad (5.3.22)$$

where  $\hat{q}_c^e = q_c^e + \hat{Q}_c^e$ . For simplicity, but without loss of generality, we will assume that  $\hat{Q}_c^e = 0$  (i.e., no external point force is placed at the center of the element) so that  $\hat{q}_c^e = q_c^e$ . Note that the load vector is equivalent to that of the Euler–Bernoulli beam element [see Eq. (5.2.18)]. In fact, for uniform load  $q$ , the load vector in Eq. (5.3.22) is identical to the one in (5.2.18). Thus, the CIE-1 element, for all analysis steps, is exactly the same as that shown in Fig. 5.3.2 with the element equations given by (5.3.22). However, one must keep in mind that  $w$  and  $q_i^e$  are determined by quadratic interpolations functions.

The second consistent interpolation element, denoted CIE-2, is based on Lagrange cubic interpolation of  $w(x)$  and quadratic interpolation of  $\Psi(x)$ . However, this element leads to  $7 \times 7$  element stiffness matrix with seven degrees of freedom ( $w_1^e, w_2^e, w_3^e, w_4^e, S_1^e, S_2^e, S_3^e$ ) per element. Elimination of the internal nodal degrees of freedom will result in a  $4 \times 4$  matrix. Alternatively, the same element can be derived directly by assuming Hermite cubic interpolation of  $w(x)$  and a *dependent* quadratic interpolation of  $\Psi(x)$ . This approach leads to an element that yields, as a special case, the Euler–Bernoulli beam element [see Reddy (1997, 2000)]. The derivation is presented here for the case  $c_f^e = 0$ .

The exact solution of Eqs. (5.3.2a) and (5.3.2b) for the homogeneous case (i.e.,  $q = 0$ ) and when  $c_f = 0$  is

$$w(x) = -\frac{1}{EI} \left( c_1 \frac{x^3}{6} + c_2 \frac{x^2}{2} + c_3 x + c_4 \right) + \frac{1}{GAK_s} (c_1 x) \quad (5.3.23a)$$

$$EI\Psi(x) = c_1 \frac{x^2}{2} + c_2 x + c_3 \quad (5.3.23b)$$

where  $c_1$  through  $c_4$  are the constants of integration. Note that the constants  $c_1, c_2$ , and  $c_3$  appearing in (5.3.23b) are the same as those in Eq. (5.3.23a). This suggests that one may use cubic approximation of  $w(x)$  and an *interdependent* quadratic approximation of  $\Psi(x)$ . The resulting finite element model is termed an *interdependent interpolation element* (IIE).

Since the solutions in (5.3.23a) and (5.3.23b) are valid also for a typical finite element (replace  $c_i$  with  $c_i^e$ ), we proceed to express  $c_i^e$  in terms of the nodal values of  $w$  and  $\Psi$ .

The resulting four relations among  $(w_1^e, w_2^e, S_1^e, S_2^e)$  and  $(c_1^e, c_2^e, c_3^e, c_4^e)$ , when inverted and substituted back into Eqs. (5.3.23a) and (5.3.24b), give

$$w(x) \approx w_h^e(x) = \sum_{j=1}^m \bar{\phi}_j^e \Delta_j^e, \quad \Psi(x) \approx \Psi_h^e(x) = \sum_{j=1}^n \varphi_j^e \Delta_j^e \quad (5.3.24a)$$

$$\Delta_1^e = w_1^e, \quad \Delta_2^e = S_1^e, \quad \Delta_3^e = w_2^e, \quad \Delta_4^e = S_2^e \quad (5.3.24b)$$

where  $\bar{\phi}_i^e$  and  $\varphi_i^e$  are the approximation functions

$$\begin{aligned} \bar{\phi}_1^e &= \frac{1}{\mu_e} [\mu_e - 12\Lambda_e \bar{x} - (3 - 2\bar{x})\bar{x}^2] \\ \bar{\phi}_2^e &= -\frac{h_e}{\mu_e} [(1 - \bar{x})^2 \bar{x} + 6\Lambda_e (1 - \bar{x}) \bar{x}] \\ \bar{\phi}_3^e &= \frac{1}{\mu_e} [(3 - 2\bar{x})\bar{x}^2 + 12\Lambda_e \bar{x}] \\ \bar{\phi}_4^e &= \frac{h_e}{\mu_e} [(1 - \bar{x})\bar{x}^2 + 6\Lambda_e (1 - \bar{x}) \bar{x}] \\ \varphi_1^e &= \frac{6}{h_e \mu_e} (1 - \bar{x}) \bar{x} \\ \varphi_2^e &= \frac{1}{\mu_e} (\mu_e - 4\bar{x} + 3\bar{x}^2 - 12\Lambda_e \bar{x}) \\ \varphi_3^e &= -\frac{6}{h_e \mu_e} (1 - \bar{x}) \bar{x} \\ \varphi_4^e &= \frac{1}{\mu_e} (3\bar{x}^2 - 2\bar{x} + 12\Lambda_e \bar{x}) \end{aligned} \quad (5.3.25a) \quad (5.3.25b)$$

Here,  $\bar{x}$  is the nondimensional local coordinate

$$\bar{x} = \frac{x - x_a}{h_e}, \quad \mu_e = 1 + 12\Lambda_e, \quad \Lambda_e = \frac{E_e I_e}{G_e A_e K_s h_e^2} \quad (5.3.26)$$

Note that the Hermite cubic interpolation functions  $\phi_i^e(x)$  of Eq. (5.2.11) are a special case of  $\bar{\phi}_i^e$ , i.e.,  $\phi_i^e$  can be obtained from  $\bar{\phi}_i^e$  by setting  $\Lambda_e = 0$  (hence,  $\mu_e = 1$ ).

Substitution of Eq. (5.3.24a) into the total potential energy functional in (5.3.7) and differentiating it with respect to  $\Delta_i^e$  yields the finite element model

$$[K^e]\{\Delta^e\} = \{q^e\} + \{Q^e\} \quad (5.3.27a)$$

where

$$\begin{aligned} K_{ij}^e &= \int_{x_a}^{x_b} \left[ E_e I_e \frac{d\varphi_i^e}{dx} \frac{d\varphi_j^e}{dx} + G_e A_e K_s \left( \varphi_i^e + \frac{d\bar{\phi}_i^e}{dx} \right) \left( \varphi_j^e + \frac{d\bar{\phi}_j^e}{dx} \right) \right] dx \\ q_i^e &= \int_{x_a}^{x_b} \bar{\phi}_i^e q(x) dx \end{aligned} \quad (5.3.27b)$$

and  $Q_i^e$  have the same meaning as before [see Eq. (5.3.4)]. Equation (5.3.27a) has the explicit form

$$\left( \frac{2E_e I_e}{\mu_e h_e^3} \right) \begin{bmatrix} 6 & -3h_e & -6 & -3h_e \\ -3h_e & 2h_e^2 \Sigma_e & 3h_e & h_e^2 \Theta_e \\ -6 & 3h_e & 6 & 3h_e \\ -3h_e & h_e^2 \Theta_e & 3h_e & 2h_e^2 \Sigma_e \end{bmatrix} \begin{Bmatrix} w_1^e \\ S_1^e \\ w_2^e \\ S_2^e \end{Bmatrix} = \begin{Bmatrix} q_1^e \\ q_2^e \\ q_3^e \\ q_4^e \end{Bmatrix} + \begin{Bmatrix} Q_1^e \\ Q_2^e \\ Q_3^e \\ Q_4^e \end{Bmatrix} \quad (5.3.28a)$$

where

$$\Lambda_e = \frac{E_e I_e}{G_e A_e K_s h_e^2}, \quad \mu_e = 1 + 12\Lambda_e, \quad \Theta_e = 1 - 6\Lambda_e, \quad \Sigma_e = 1 + 3\Lambda_e \quad (5.3.28b)$$

For uniformly distributed load,  $q(x) = q_0$ , the load vector in (5.3.27b) yields

$$\{q^e\} = \frac{q_0 h_e}{12} \begin{Bmatrix} 6 \\ -h_e \\ 12 \\ h_e \end{Bmatrix} \quad (5.3.28c)$$

which is exactly the same as that in the Euler–Bernoulli beam element (EBE). Of course, for nonuniform loads the load vectors of the two elements are different.

In the thin beam limit (i.e.,  $\Lambda_e \rightarrow 0$ ), Eq. (5.3.28a) reduces to the EBE equations (5.2.17) and (5.2.18) (with  $c_f^e = 0$ ). The IIE element leads to the exact nodal values for any distribution of the transverse load  $q(x)$  provided that the bending stiffness  $EI$  and shear stiffness  $K_s GA$  are elementwise constant (and  $c_f = 0$ ). Such an element is said to be *superconvergent*. Note that the bar element and EBE are also superconvergent elements (i.e., bar element, IIE, and EBE yield exact nodal values of the respective theories).

### 5.3.5 Reduced Integration Element

When equal interpolation of  $w(x)$  and  $\Psi(x)$  is used ( $m = n$ ), all submatrices in (5.3.16) are of the same order:  $n \times n$ , where  $n$  is the number of terms in the polynomial (or  $n - 1$  is the degree of interpolation). The element coefficient matrices  $K_{ij}^{11}$ ,  $K_{ij}^{12}$  as well as the first part of  $K_{ij}^{22}$  must be evaluated exactly. The second part of  $K_{ij}^{22}$  is to be evaluated using reduced integration. For the choice of linear interpolation functions, and for elementwise constant values of  $GAK_s$  and  $EI$ , the matrices have the following explicit values (when  $c_f^e = 0$ ):

$$\begin{aligned} [K^{11}] &= \frac{G_e A_e K_s}{h_e} \begin{bmatrix} 1 & -1 \\ -1 & 1 \end{bmatrix}, \quad [K^{12}] = \frac{G_e A_e K_s}{2} \begin{bmatrix} -1 & -1 \\ 1 & 1 \end{bmatrix} \\ [K^{22}] &= \frac{E_e I_e}{h_e} \begin{bmatrix} 1 & -1 \\ -1 & 1 \end{bmatrix} + \frac{G_e A_e K_s h_e}{4} \begin{bmatrix} 1 & 1 \\ 1 & 1 \end{bmatrix} \end{aligned} \quad (5.3.29)$$

where one-point integration is used to evaluate the second part of  $[K^{22}]$ . Note that  $[K^{11}]$ ,  $[K^{12}]$ , and the first part of  $[K^{22}]$  can be evaluated exactly with one-point quadrature (i.e., numerical integration) when  $EI$  and  $GAK_s$  are constant because the integrands of these coefficients are constant. Hence, one-point integration for  $[K^{\alpha\beta}]$  satisfies all the requirements. The resulting beam element is termed the reduced integration element (RIE).

The element equations of the RIE are ( $\alpha_e = 4E_e I_e / G_e A_e K_s$ )

$$\frac{G_e A_e K_s}{4h_e} \begin{bmatrix} 4 & -2h_e & -4 & -2h_e \\ -2h_e & h_e^2 + \alpha_e & 2h_e & h_e^2 - \alpha_e \\ -4 & 2h_e & 4 & 2h_e \\ -2h_e & h_e^2 - \alpha_e & 2h_e & h_e^2 + \alpha_e \end{bmatrix} \begin{Bmatrix} w_1^e \\ S_1^e \\ w_2^e \\ S_2^e \end{Bmatrix} = \begin{Bmatrix} Q_1^e \\ Q_2^e \\ Q_3^e \\ Q_4^e \end{Bmatrix} + \begin{Bmatrix} q_1^e \\ 0 \\ q_2^e \\ 0 \end{Bmatrix} \quad (5.3.30a)$$

or, in alternative form (to resemble those of the EBE)

$$\frac{2E_e I_e}{\mu_0 h_e^3} \begin{bmatrix} 6 & -3h_e & -6 & -3h_e \\ -3h_e & h_e^2(1.5 + 6\Lambda_e) & 3h_e & h_e^2(1.5 - 6\Lambda_e) \\ -6 & 3h_e & 6 & 3h_e \\ -3h_e & h_e^2(1.5 - 6\Lambda_e) & 3h_e & h_e^2(1.5 + 6\Lambda_e) \end{bmatrix} \begin{Bmatrix} w_1^e \\ S_1^e \\ w_2^e \\ S_2^e \end{Bmatrix} = \begin{Bmatrix} q_1^e \\ 0 \\ q_2^e \\ 0 \end{Bmatrix} + \begin{Bmatrix} Q_1^e \\ Q_2^e \\ Q_3^e \\ Q_4^e \end{Bmatrix} \quad (5.3.30b)$$

where

$$q_i^e = \int_{x_a}^{x_b} \psi_i^e q \, dx, \quad (i = 1, 2) \quad (5.3.31)$$

$$\Lambda_e = \frac{E_e I_e}{G_e A_e K_s h_e^2}, \quad \mu_0 = 12\Lambda_e \quad (5.3.32)$$

and  $\psi_i$  are the linear interpolation functions.

It is interesting to note that the element stiffness matrix (5.3.30b) of the linear RIE is the same as that of the CIE-1 in (5.3.22) obtained using quadratic approximation of  $w$  and linear approximation of  $\Psi$ . The only difference is the load representation. In CIE-1, the load vector is equivalent to that of the Euler–Bernoulli beam theory, whereas in RIE it is based on (5.3.31), which contributes only to the force degrees of freedom and not to the moment degrees of freedom.

The quadratic interpolation of both  $w$  and  $\Psi$  with full integration of the element coefficient matrices also suffers slightly from the shear-locking phenomenon. A uniform two-point quadrature rule has the desired effect on  $[K^{11}]$ ,  $[K^{12}]$ , and  $[K^{22}]$ , i.e.,  $[K^{11}]$ ,  $[K^{12}]$ , and the first term of  $[K^{22}]$  will be evaluated exactly and the second term of  $[K^{22}]$  approximately. As the degree of approximation and/or the number of elements in the mesh is increased, shear locking will disappear and reduced integration is not necessary.

### 5.3.6 Numerical Examples

#### Example 5.3.1

Consider a simply supported beam under distributed transverse load of intensity  $q_0$ . The following data is used in computing the numerical values:

$$E = 10^6, \quad \nu = 0.25, \quad K_s = \frac{5}{6}, \quad q_0 = 1, \quad I = \frac{bH^3}{12}, \quad A = bH, \quad b = 1$$

**Table 5.3.1** Comparison of the finite element solutions with the exact maximum deflection and rotation of a simply supported isotropic beam of Example 5.3.1.

Element	$N^* = 1$	$N = 2$	$N = 4$	$N = 1$	$N = 2$	$N = 4$
	$w(L/2) \times (EH^3/q_0L^4)$			$-\Psi(0) \times 10^3$		
	<i>Uniform load (<math>L/H = 10</math>)</i>					
<b>RIE</b>	0.09750	0.14438	0.15609	0.37500	0.46875	0.49219
<b>CIE-I</b>	0.12875	0.15219	0.15805	0.50000	0.50000	0.50000
<b>IIE<sup>†</sup></b>	0.16000	0.16000	0.16000	0.50000	0.50000	0.50000
<b>EBE<sup>†</sup></b>	0.15625	0.15625	0.15625	0.50000	0.50000	0.50000
	<i>Uniform load (<math>L/H = 100</math>)</i>					
<b>RIE</b>	0.09379	0.14066	0.15238	0.37500	0.46875	0.49219
<b>CIE-I</b>	0.12504	0.14847	0.15433	0.50000	0.50000	0.50000
<b>IIE<sup>†</sup></b>	0.15629	0.15629	0.15629	0.50000	0.50000	0.50000
<b>EBE<sup>†</sup></b>	0.15625	0.15625	0.15625	0.50000	0.50000	0.50000
	<i>Sinusoidal load (<math>L/H = 100</math>)</i>					
<b>RIE</b>	0.07639	0.11079	0.12007	0.30543	0.36702	0.38204
<b>CIE-I</b>	0.09679	0.11682	0.12163	0.38705	0.38702	0.38702
<b>IIE<sup>†</sup></b>	0.12322	0.12322	0.12322	0.38702	0.38702	0.38702
<b>EBE<sup>†</sup></b>	0.12319	0.12319	0.12319	0.38702	0.38702	0.38702

\*  $N$  is the number of elements used in the half beam.

† Exact values compared to the respective beam theories.

Two different beam length-to-height ratios,  $L/H = 10$  and  $L/H = 100$ , are considered. Table 5.3.1 shows a comparison of the finite element solutions obtained with one, two, and four elements in half beam with the exact beam solutions for two different types of loads, namely, uniform load and sinusoidal load. The exact solutions according to the two theories are given below [see Wang et al. (2000)].

### Euler-Bernoulli Beam Theory

$$\text{Uniform Load} \quad w^E(x) = \frac{q_0 L^4}{24EI} (\bar{x} - 2\bar{x}^3 + \bar{x}^4) \quad (5.3.33)$$

$$\text{Sinusoidal Load} \quad w^E(x) = \frac{16q_0 L^4}{\pi EI} \sin \pi \bar{x}, \quad \bar{x} = \frac{x}{L}$$

### Timoshenko Beam Theory

#### Uniform Load

$$w^T(x) = \left[ w^E(x) + \frac{1}{GAK_s} M^E(x) \right] = \frac{q_0 L^4}{24EI} (\bar{x} - 2\bar{x}^3 + \bar{x}^4) + \frac{q_0 L^2}{2GAK_s} (\bar{x} - \bar{x}^3)$$

$$\Psi(x) = -\frac{dw^E}{dx} = -\frac{q_0 L^3}{24EI} (1 - 6\bar{x}^2 + 4\bar{x}^3), \quad \bar{x} = \frac{x}{L} \quad (5.3.34)$$

#### Sinusoidal Load

$$w^T(x) = \left[ w^E(x) + \frac{1}{GAK_s} M^E(x) \right] = \left( \frac{16q_0 L^4}{\pi EI} + \frac{16\pi q_0 L^2}{GAK_s} \right) \sin \pi \bar{x}$$

$$\Psi(x) = -\frac{dw^E}{dx} = -\frac{16q_0 L^3}{EI} \cos \pi \bar{x}, \quad \bar{x} = \frac{x}{L} \quad (5.3.35)$$

where the superscripts  $E$  and  $T$  refer to the Euler–Bernoulli and Timoshenko beam theories, respectively. Clearly, more than two elements of CIE-1 and RIE are required to obtain acceptable solutions. On the other hand, IIE yields exact nodal values with one element (because it is a superconvergent element).

### Example 5.3.2

Consider the cantilever beam of Example 5.2.1. We wish to analyze the problem using various Timoshenko beam finite elements. The problem data is given in (5.2.33);  $\nu = 0.25$ ,  $K_s = 5/6$ . The exact solution of the problem according to the Timoshenko beam theory is given by [see Wang et al. (2000)]

$$w^T(x) = w^E(x) + GAK_s [M^E(x) - M^E(0)], \quad \Psi(x) = -\frac{dw^E}{dx}$$

where again the superscripts  $E$  and  $T$  refer to the Euler–Bernoulli and Timoshenko beam theories, respectively. Table 5.3.2 contains the end deflection  $w(L)$  and end rotation  $\Psi(L)$  for two, four, and eight elements in full beam.

To further understand the effect of shear locking, we consider Timoshenko beam elements with equal interpolation of  $w$  and  $\Psi$ . Linear as well as quadratic elements with and without reduced integration are tested and the results are included in Table 5.3.3. It is clear that the *full integration elements* (FIEs) produce erroneous results, implying that shear locking is present. Shear locking gradually vanishes as the mesh is refined with either linear elements or quadratic elements.

The following general observations can be made about various finite element models based on the Timoshenko beam theory:

1. The RIE exhibits less locking compared with the FIE.
2. As the number of elements in the mesh is increased or the degree of approximation is increased (i.e., higher-order elements are used), the finite element solutions obtained by both RIE and FIE improve; i.e., the effect of locking is reduced with mesh refinements and with the use of higher-order elements.

**Table 5.3.2** Comparison of the finite element solutions obtained with various types of finite elements for the cantilever beam of Example 5.3.2.

$N$	$w(L)$ (m)				$-\Psi(L)$			
	EBE	RIE	CIE-1	IIE	EBE	RIE	CIE-1	IIE
Thin beam, $H = 0.0703$ ( $w$ and $\Psi$ )								
2	0.1043	0.0995	0.0974	0.1043	0.0512	0.0524	0.0512	0.0512
4	0.1043	0.1031	0.1026	0.1043	0.0512	0.0515	0.0512	0.0512
8	0.1043	0.1040	0.1039	0.1043	0.0512	0.0513	0.0512	0.0512
Thick beam, $H = 0.3$ ( $w \times 10^2$ and $\Psi \times 10^3$ )								
2	0.1344	0.1293	0.1265	0.1355	0.6600	0.6750	0.6600	0.6600
4	0.1344	0.1340	0.1332	0.1355	0.6600	0.6638	0.6600	0.6600
8	0.1344	0.1351	0.1349	0.1355	0.6600	0.6609	0.6600	0.6600

<sup>†</sup> For EBE,  $\Psi = \theta \equiv -dw/dx$ .

**Table 5.3.3** Effect of reduced integration of transverse shear coefficients on the deflections of the cantilever beam of Example 5.3.2.

Element	Linear			Quadratic		
	$N = 2$	$N = 4$	$N = 8$	$N = 1$	$N = 2$	$N = 4$
Thin beam, $H = 0.0703$ (exact $w = 0.1043$ )						
RIE ( $2 \times 1$ ) <sup>†</sup>	0.0995	0.1031	0.1040	0.1048	0.1043	0.1043
FIE ( $2 \times 2$ )	0.0007	0.0027	0.0100	0.0771	0.0976	0.1028
Thick beam, $H = 0.3$ (exact $w \times 10^2 = 0.1355$ )						
RIE ( $3 \times 2$ )	0.1293	0.1340	0.1351	0.1361	0.1355	0.1355
FIE ( $3 \times 3$ )	0.0148	0.0442	0.0892	0.1048	0.1299	0.1348

<sup>†</sup> Gauss integration rule used to evaluate bending and shear terms.

3. The IIE (i.e., Hermite cubic approximation of  $w$  and a dependent quadratic approximation of  $\Psi$ ) with full integration yields exact nodal values.
4. The element with quadratic approximation of both  $w$  and  $\Psi$  and reduced integration of the coefficients yields more accurate results than the CIE with quadratic approximation of  $w$  and the linear approximation of  $\Psi$  and with full integration of the coefficients.
5. The IIE is the best element for the analysis of bending beams as it contains the EBE as a special case; IIE automatically takes into account the transverse shear deformation if it is significant.

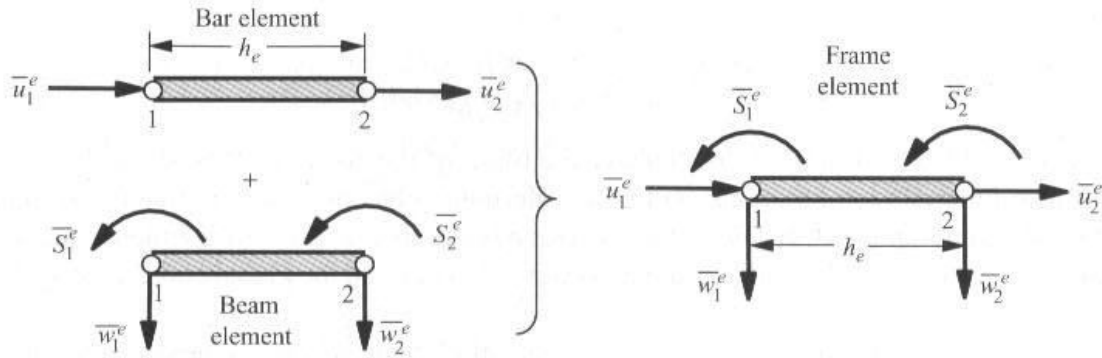
## 5.4 PLANE FRAME ELEMENTS

### 5.4.1 Introductory Comments

Recall that a bar element oriented arbitrarily in a plane is called a truss element. A plane truss element contains two degrees of freedom per node ( $u, v$ ), an axial ( $u$ ) and transverse displacement ( $v$ ). By definition, a bar element can carry only axial loads and deform axially, whereas beams can take transverse loads and bending moments about an axis perpendicular to the plane of the member. A superposition of bar and beam degrees of freedom gives a finite element that is known as a frame element (see Fig. 5.4.1). Members of a frame structure are connected by rigid connections (e.g., welded or riveted), and therefore axial and transverse forces and bending moments are developed in the members. The objective of this section is to formulate a frame finite element, with the help of the developments from Sections 4.6, 5.2, and 5.3.

### 5.4.2 Frame Element

In many truss and frame structures, the bar and beam structural elements are found in many different orientations (see, for example, Fig. 4.6.1). Analysis of such structures for displacements and stresses requires the setting up of a global coordinate system and referencing all quantities (i.e., displacements, forces, and stiffnesses) of individual elements to the common (global) coordinate system in order to assemble the elements and impose boundary conditions on the whole structure.



**Figure 5.4.1** Superposition of bar and beam element to obtain a frame element [degrees of freedom are referred to the element coordinate system  $(\bar{x}, \bar{y}, \bar{z})$ ].

A superposition of the bar element of Section 4.6 with the EBE of Section 5.2 or the Timoshenko beam element (RIE, CIE, or IIE) of Section 5.3 gives a frame element with three primary degrees of freedom ( $u, w, S$ ) per node (note that the transverse displacement  $v$  of Section 4.6 is now denoted by  $w$  to be consistent with Sections 5.2 and 5.3). When the axial stiffness  $EA$  and bending stiffness  $EI$  are elementwise constant, the superposition of the linear bar element with the IIE gives the following element equations (see Fig. 5.4.1):

$$[\bar{K}]^e \{\bar{\Delta}\}^e = \{\bar{F}\}^e \quad (5.4.1a)$$

or, in explicit form,

$$\frac{2EI}{\mu_0 h^3} \begin{bmatrix} \mu & 0 & 0 & -\mu & 0 & 0 \\ 0 & 6 & -3h & 0 & -6 & -3h \\ 0 & -3h & h^2(1.5 + 6\Lambda) & 0 & 3h & h^2(1.5 - 6\Lambda) \\ -\mu & 0 & 0 & \mu & 0 & 0 \\ 0 & -6 & 3h & 0 & 6 & 3h \\ 0 & -3h & h^2(1.5 - 6\Lambda) & 0 & 3h & h^2(1.5 + 6\Lambda) \end{bmatrix}^e \begin{Bmatrix} \bar{u}_1 \\ \bar{w}_1 \\ \bar{S}_1 \\ \bar{u}_2 \\ \bar{w}_2 \\ \bar{S}_2 \end{Bmatrix}^e = \begin{Bmatrix} \bar{F}_1 \\ \bar{F}_2 \\ \bar{F}_3 \\ \bar{F}_4 \\ \bar{F}_5 \\ \bar{F}_6 \end{Bmatrix}^e \quad (5.4.1b)$$

where

$$\begin{Bmatrix} \bar{F}_1 \\ \bar{F}_2 \\ \bar{F}_3 \\ \bar{F}_4 \\ \bar{F}_5 \\ \bar{F}_6 \end{Bmatrix}^e = \begin{Bmatrix} \bar{f}_1 \\ \bar{q}_1 \\ \bar{q}_2 \\ \bar{f}_2 \\ \bar{q}_3 \\ \bar{q}_4 \end{Bmatrix}^e + \begin{Bmatrix} \bar{Q}_1 \\ \bar{Q}_2 \\ \bar{Q}_3 \\ \bar{Q}_4 \\ \bar{Q}_5 \\ \bar{Q}_6 \end{Bmatrix}^e \quad (5.4.2a)$$

$$\bar{f}_i = \int_0^{h_e} f^e(\bar{x}) \psi_i^e(\bar{x}) d\bar{x} \quad (i = 1, 2), \quad \bar{q}_i = \int_0^{h_e} q^e(\bar{x}) \phi_i^e(\bar{x}) d\bar{x} \quad (i = 1, 2, 3, 4) \quad (5.4.2b)$$

and

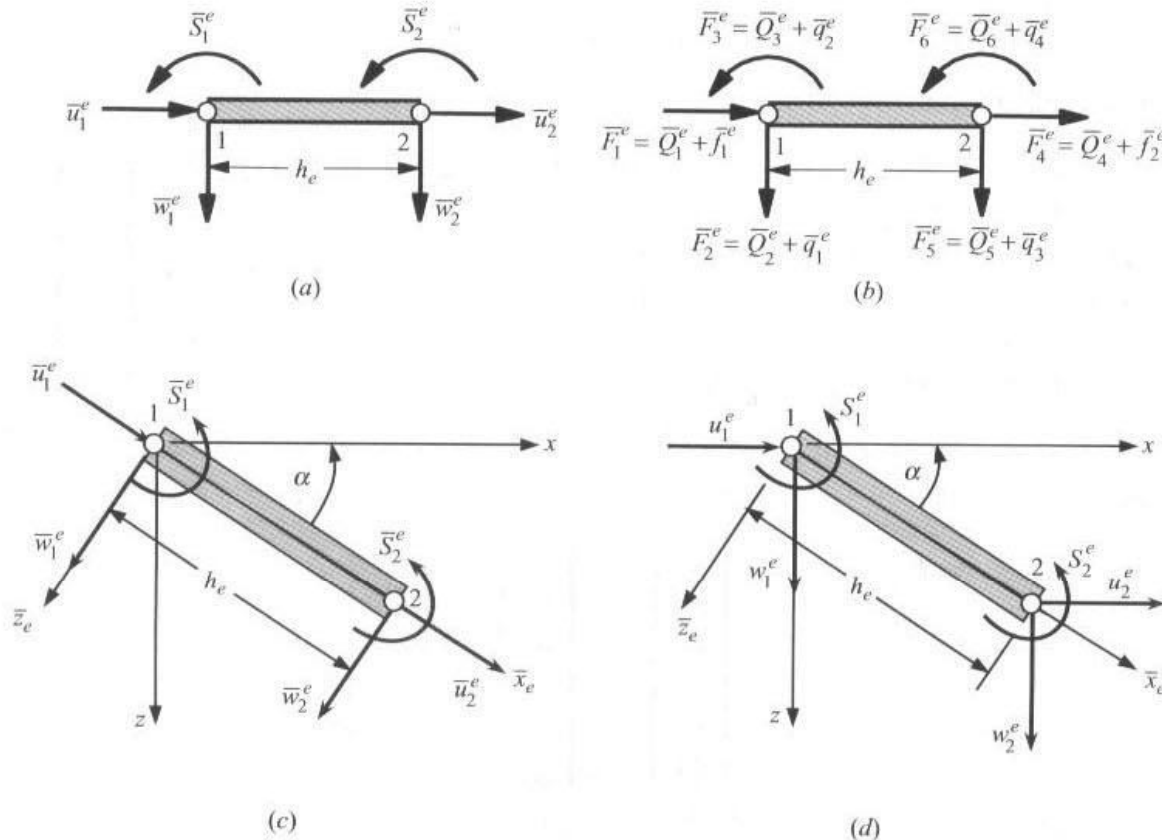
$$\mu = \frac{A\mu_0 h^2}{2I}, \quad \Lambda = \frac{EI}{GAK_s h^2}, \quad \mu_0 = 12\Lambda \quad (5.4.3)$$

In Eq. (5.4.2b),  $f^e$  denotes the distributed axial force,  $q^e$  the distributed transverse force,  $\psi_i^e$  the linear interpolation functions, and  $\phi_i^e$  the Hermite cubic interpolation functions. In the following paragraphs, we develop transformation relations to express the element equations (5.4.1b)—valid in the element coordinate system  $(\bar{x}, \bar{y}, \bar{z})$ —to the global coordinate system  $(x, y, z)$ .

The local coordinates  $(\bar{x}_e, \bar{y}_e, \bar{z}_e)$  of a typical element  $\Omega_e$  are related to the global coordinates  $(x, y, z)$  by [cf. Eq. (4.6.2)]

$$\begin{Bmatrix} \bar{x} \\ \bar{y} \\ \bar{z} \end{Bmatrix}^e = \begin{bmatrix} \cos \alpha & 0 & \sin \alpha \\ 0 & 1 & 0 \\ -\sin \alpha & 0 & \cos \alpha \end{bmatrix}^e \begin{Bmatrix} x \\ y \\ z \end{Bmatrix} \quad (5.4.4)$$

where the angle  $\alpha_e$  is measured clockwise from the global  $x$ -axis to the element  $\bar{x}_e$ -axis. Note that the  $y$  and  $\bar{y}_e$  coordinates are parallel to each other, and they are *out of* the plane of the paper (see Fig. 5.4.2). The same transformation relations hold for displacements  $(u, w)$  along the global coordinates  $(x, z)$  and displacements  $(\bar{u}, \bar{w})$  in the local coordinates



**Figure 5.4.2** (a) Generalized displacements. (b) Generalized forces. (c) Generalized displacements in the element coordinates. (d) Generalized displacements in the global coordinates.

$(\bar{x}, \bar{z})$ . Note that there is no displacement in the direction of the coordinate  $y$  (i.e.,  $v = 0$ ). However, there is a rotation about the  $y$ -axis, and it remains the same in both coordinate systems because  $y = \bar{y}$ . Note that rotation  $\theta$  is equal to  $-dw/dx$  in Euler–Bernoulli beam theory and it is equal to  $\Psi$  in Timoshenko beam theory. Hence, the relationship between  $(u, w, \theta)$  and  $(\bar{u}, \bar{w}, \bar{\theta})$  can be written as

$$\begin{Bmatrix} \bar{u} \\ \bar{w} \\ \bar{\theta} \end{Bmatrix}^e = \begin{bmatrix} \cos \alpha & \sin \alpha & 0 \\ -\sin \alpha & \cos \alpha & 0 \\ 0 & 0 & 1 \end{bmatrix}^e \begin{Bmatrix} u \\ w \\ \theta \end{Bmatrix}^e \quad (5.4.5)$$

Therefore, the three nodal degrees of freedom  $(\bar{u}_i^e, \bar{w}_i^e, \bar{S}_i^e)$  at the  $i$ th node ( $i = 1, 2$ ) in the  $(\bar{x}, \bar{y}, \bar{z})$  system are related to the three degrees of freedom  $(u_i^e, w_i^e, S_i^e)$  in the  $(x, y, z)$  system by

$$\begin{Bmatrix} \bar{u}_1 \\ \bar{w}_1 \\ \bar{S}_1 \\ \bar{u}_2 \\ \bar{w}_2 \\ \bar{S}_2 \end{Bmatrix}^e = \begin{bmatrix} \cos \alpha & \sin \alpha & 0 & & & \\ -\sin \alpha & \cos \alpha & 0 & & & \\ 0 & 0 & 1 & & & \\ & & & \cos \alpha & \sin \alpha & 0 \\ & & & -\sin \alpha & \cos \alpha & 0 \\ & & & 0 & 0 & 1 \end{bmatrix}^e \begin{Bmatrix} u_1 \\ w_1 \\ S_1 \\ u_2 \\ w_2 \\ S_2 \end{Bmatrix}^e \quad (5.4.6a)$$

or

$$\{\bar{\Delta}^e\} = [T^e]\{\Delta^e\} \quad (5.4.6b)$$

Analogously, the element force vectors in the local and global coordinate systems are related according to

$$\{\bar{F}^e\} = [T]^e\{F^e\} \quad (5.4.7)$$

Returning to Eq. (5.4.1a), we substitute the transformation equations (5.4.6b) and (5.4.7) into (5.4.1a) and obtain

$$[\bar{K}]^e [T]^e \{\Delta\}^e = [T]^e \{F\}^e$$

Premultiplying both sides with  $[T]^{-1} = [T]^T$ , we obtain

$$[T]^T [\bar{K}]^e [T]^e \{\Delta\}^e = \{F\}^e \quad \text{or} \quad [K]^e \{\Delta\}^e = \{F\}^e \quad (5.4.8)$$

where

$$[K^e] = [T]^T [\bar{K}]^e [T]^e, \quad \{F\}^e = [T]^T \{\bar{F}\}^e \quad (5.4.9)$$

Thus, if we know the element matrices  $[\bar{K}]^e$  and  $\{\bar{F}\}^e$  of an element  $\Omega_e$  in the local coordinate system  $(\bar{x}, \bar{y}, \bar{z})$ , the element matrices in the global coordinate system are obtained by (5.4.9).

Using  $[\bar{K}]^e$  and  $\{\bar{F}\}^e$  from Eq. (5.4.1b) in (5.4.9) and carrying out the indicated matrix multiplications, we arrive at the following element stiffness matrix  $[K^e]$  referred to the

global coordinates:

$$[K]^e = \frac{2EI}{\mu_0 h^3} \begin{bmatrix} \mu \cos^2 \alpha + 6 \sin^2 \alpha & (\mu - 6) \cos \alpha \sin \alpha & 3h \sin \alpha \\ (\mu - 6) \cos \alpha \sin \alpha & \mu \sin^2 \alpha + 6 \cos^2 \alpha & -3h \cos \alpha \\ 3h \sin \alpha & -3h \cos \alpha & h^2(1.5 + 6\Lambda) \\ -(\mu \cos^2 \alpha + 6 \sin^2 \alpha) & -(\mu - 6) \sin \alpha \cos \alpha & -3h \sin \alpha \\ -(\mu - 6) \cos \alpha \sin \alpha & -(\mu \sin^2 \alpha + 6 \cos^2 \alpha) & 3h \cos \alpha \\ 3h \sin \alpha & -3h \cos \alpha & h^2(1.5 - 6\Lambda) \\ -(\mu \cos^2 \alpha + 6 \sin^2 \alpha) & -(\mu - 6) \cos \alpha \sin \alpha & 3h \sin \alpha \\ -(\mu - 6) \sin \alpha \cos \alpha & -(\mu \sin^2 \alpha + 6 \cos^2 \alpha) & -3h \cos \alpha \\ -3h \sin \alpha & 3h \cos \alpha & h^2(1.5 - 6\Lambda) \\ (\mu \cos^2 \alpha + 6 \sin^2 \alpha) & (\mu - 6) \cos \alpha \sin \alpha & -3h \sin \alpha \\ (\mu - 6) \cos \alpha \sin \alpha & \mu \sin^2 \alpha + 6 \cos^2 \alpha & 3h \cos \alpha \\ -3h \sin \alpha & 3h \cos \alpha & h^2(1.5 + 6\Lambda) \end{bmatrix} \quad (5.4.10a)$$

$$\{F\}^e = \begin{Bmatrix} F_1 \\ F_2 \\ F_3 \\ F_4 \\ F_5 \\ F_6 \end{Bmatrix}^e = \begin{Bmatrix} \bar{F}_1 \cos \alpha - \bar{F}_2 \sin \alpha \\ \bar{F}_1 \sin \alpha + \bar{F}_2 \cos \alpha \\ \bar{F}_3 \\ \bar{F}_4 \cos \alpha - \bar{F}_5 \sin \alpha \\ \bar{F}_4 \sin \alpha + \bar{F}_5 \cos \alpha \\ \bar{F}_6 \end{Bmatrix}^e \quad (5.4.10b)$$

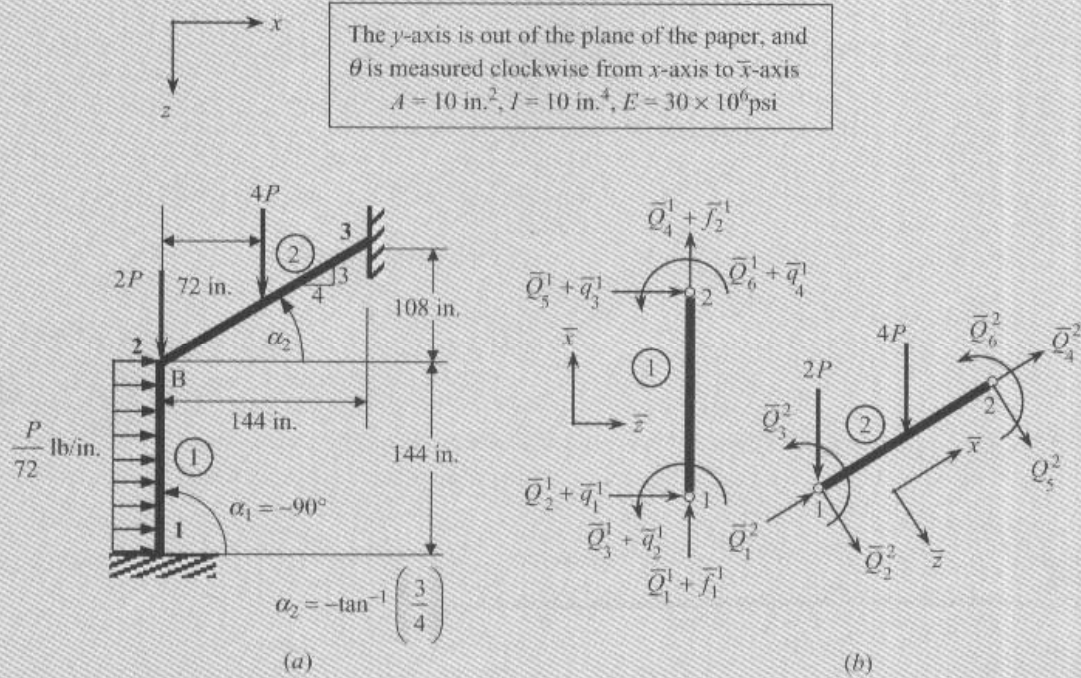
which is the element force vector referred to the global coordinates.

### Example 5.4.1

The frame structure shown in Fig. 5.4.3 is to be analyzed for displacements and forces. Both members of the structure are made of the same material ( $E$ ) and have the same geometric properties ( $A$ ,  $I$ ). The element stiffness matrices and force vectors in the global coordinate system ( $x$ ,  $y$ ,  $z$ ) can be computed from (5.4.10a) and (5.4.10b). The geometric and material properties of each element are as follows ( $f$  is the axial and  $q$  is the transverse distributed load).

#### Element 1.

$$L = 144 \text{ in.}, \quad A = 10 \text{ in.}^2, \quad I = 10 \text{ in.}^4, \quad \cos \alpha_1 = 0.0, \quad \sin \alpha_1 = -1.0 \\ E = 10^6 \text{ psi}, \quad f^{(1)} = 0, \quad q^{(1)} = \frac{P}{72} \text{ lb/in.} \quad (5.4.11)$$



**Figure 5.4.3** (a) Geometry and loading, and (b) member forces in the plane frame structure of Example 5.4.1.

$$[K^1] = 10^5 \begin{bmatrix} 0.0004 & 0.0000 & -0.0289 & -0.0004 & 0.0000 & -0.0289 \\ 0.0000 & 0.6944 & 0.0000 & 0.0000 & -0.6944 & 0.0000 \\ -0.0289 & 0.0000 & 2.7778 & 0.0289 & 0.0000 & 1.3889 \\ -0.0004 & 0.0000 & 0.0289 & 0.0004 & 0.0000 & 0.0289 \\ 0.0000 & -0.6944 & 0.0000 & 0.0000 & 0.6944 & 0.0000 \\ -0.0289 & 0.0000 & 1.3889 & 0.0289 & 0.0000 & 2.7778 \end{bmatrix}$$

$$\{f^1\} = P\{1.0 \quad 0.0 \quad -24.0 \quad 1.0 \quad 0.0 \quad 24.0\}^T$$

#### Element 2.

$$L = 180 \text{ in.}, \quad A = 10 \text{ in.}^2, \quad I = 10 \text{ in.}^4, \quad \cos \alpha_2 = 0.8, \quad \sin \alpha_2 = -0.6$$

$$E = 10^6 \text{ psi}, \quad f^{(2)} = 0, \quad q^{(2)} = 0 \quad (5.4.12)$$

The load  $F_0 = 4P$  at the center of the element ( $\cos \alpha = -0.6$  and  $\sin \alpha = 0.8$ ) is distributed to the nodes according to Eq. (5.2.20).

$$[K^2] = 10^5 \begin{bmatrix} 0.3556 & -0.2666 & -0.0111 & -0.3556 & 0.2666 & -0.0111 \\ -0.2666 & 0.2001 & -0.0148 & 0.2666 & -0.2001 & -0.0148 \\ -0.0111 & 0.0148 & 2.2222 & 0.0111 & 0.0148 & 1.1111 \\ -0.3556 & 0.2666 & 0.0111 & 0.3556 & -0.2666 & 0.0111 \\ 0.2666 & -0.2001 & 0.0148 & -0.2666 & 0.2001 & 0.0148 \\ -0.0111 & -0.0148 & 1.1111 & 0.0111 & 0.0148 & 2.2222 \end{bmatrix}$$

$$\{f^2\} = P\{0.0 \quad 2.0 \quad -72.0 \quad 0.0 \quad 2.0 \quad 72.0\}^T$$

The assembled stiffness matrix and force vectors are obtained by superposing the last three rows and columns of element 1 to the first three rows and columns of element 2, i.e., the  $3 \times 3$  submatrix associated with rows and columns 4, 5, and 6 of element 1, and the  $3 \times 3$  submatrix associated with rows and columns 1, 2, and 3 of element 2 overlap in the global stiffness matrix.

The known geometric boundary conditions are

$$U_1 = 0, \quad U_2 = 0, \quad U_3 = 0, \quad U_7 = 0, \quad U_8 = 0, \quad U_9 = 0 \quad (5.4.13a)$$

The force boundary conditions are

$$Q_4^1 + Q_1^2 = 0, \quad Q_5^1 + Q_2^2 = 2P, \quad Q_6^1 + Q_3^2 = 0 \quad (5.4.13b)$$

Since all specified values of the known boundary conditions on the primary variables are zero, the condensed equations for the unknown generalized displacement degrees of freedom are

$$10^5 \begin{bmatrix} 0.3560 & -0.2666 & 0.0178 \\ -0.2666 & 0.8946 & -0.0148 \\ 0.0178 & -0.0148 & 5.0000 \end{bmatrix} \begin{Bmatrix} U_4 \\ U_5 \\ U_6 \end{Bmatrix} = P \begin{Bmatrix} 1.0 \\ 2.0 \\ -4.8 \end{Bmatrix} \quad (5.4.14)$$

The solution is

$$U_4 = 0.8390 \times 10^{-4} P \text{ (in.)}, \quad U_5 = 0.6812 \times 10^{-4} P \text{ (in.)}, \quad U_6 = -0.9610 \times 10^{-4} P \text{ (rad.)} \quad (5.4.15)$$

The reactions and forces in each member in the global coordinates can be computed from the element equations

$$\{Q^e\} = [K^e]\{u^e\} - \{f^e\} \quad (5.4.16a)$$

The forces  $\{Q^e\}$  can be transformed to those in the element coordinate system by means of (5.4.7):

$$\{\bar{Q}^e\} = [T^e]\{Q^e\} \quad (5.4.16b)$$

We obtain

$$\{\bar{Q}^1\} = \begin{Bmatrix} 4.731 \\ -0.725 \\ 10.900 \\ -4.731 \\ -1.275 \\ -50.450 \end{Bmatrix} P, \quad \{\bar{Q}^2\} = \begin{Bmatrix} 2.658 \\ -1.420 \\ 50.45 \\ -0.258 \\ -1.780 \\ -82.87 \end{Bmatrix} P \quad (5.4.17)$$

Table 5.4.1 contains the displacements obtained by various types of elements at point B. As noted earlier, one EBE or IIE per member of a structure gives exact displacements, whereas at least two RIE or CIE per member are needed to obtain acceptable results. The forces in each element are included in Table 5.4.2. The forces calculated from the element equations are also exact for EBE and IIE.

**Table 5.4.1** Comparison of the generalized displacements [ $\bar{v} = (v/P) \times 10^4$  where  $v$  is a typical displacement] at point B of the frame structure shown in Fig. 5.4.3.

Displ.	RIE(1)*	RIE (2)	RIE (4)	CIE (1)	CIE (2)	CIE (4)	IIE <sup>†</sup>	EBE <sup>†</sup>
$\bar{u}_B$	0.27092	0.84765	0.84107	0.28435	0.84146	0.83959	0.83898	0.83904
$\bar{w}_B$	0.46609	0.68056	0.68108	0.44315	0.68083	0.68114	0.68123	0.68124
$-\bar{\phi}_B$	-0.0016	0.86647	0.94501	0.00036	0.77029	0.91640	0.96206	0.96098

\*Number in the parenthesis denotes the number of elements per member.

<sup>†</sup>Values are independent of the number of elements (and coincide with the exact values predicated by the respective beam theories).

**Table 5.4.2** Comparison of the generalized forces (divided by  $P$ ) in each member of the frame structure.

Element*	$\bar{Q}_1$	$-\bar{Q}_2$	$\bar{Q}_3$	$-\bar{Q}_4$	$-\bar{Q}_5$	$-\bar{Q}_6$
RIE(1)	3.237	1.865	62.24	3.237	0.136	62.26
	0.850	0.908	62.26	1.550	2.292	62.28
RIE(2)	4.723	0.671	0.332	4.723	1.329	47.70
	2.699	1.384	47.70	0.299	1.816	86.67
RIE(4)	4.730	0.713	8.362	4.730	1.288	49.76
	2.668	1.411	49.76	0.268	1.789	83.74
CIE(1)	3.077	1.575	65.39	3.077	0.425	17.38
	0.987	0.607	17.38	1.413	2.593	161.4
CIE(2)	4.728	0.708	8.327	4.728	1.292	50.37
	2.670	1.407	50.37	0.270	1.793	85.07
CIE(4)	4.730	0.721	10.30	4.730	1.279	50.43
	2.661	1.417	50.43	0.261	1.783	83.39
IIE <sup>†</sup>	4.731	0.725	10.92	4.731	1.275	50.45
	2.658	1.420	50.45	0.258	1.780	82.87
EBE <sup>†</sup>	4.731	0.725	10.90	4.731	1.275	50.45
	2.658	1.420	50.45	0.258	1.780	82.87

\*Number in the parenthesis denotes the number of elements per member, and the two rows correspond to the two members of the structure.

<sup>†</sup>Values are independent of the number of elements (and coincide with the exact values predicated by the respective beam theories).

## 5.5 SUMMARY

In this chapter, finite element models of the classical (i.e., Euler–Bernoulli) and Timoshenko beam theories have been developed. The classical beam theory is governed by a fourth-order differential equation and therefore results in a weak form whose primary variables contain the transverse deflection and its first derivative. Therefore, Hermite interpolation of the transverse deflection is required in order to impose the continuity of the deflection and its derivative at the nodes between elements. In the case of the Timoshenko beam theory, there

are two, coupled, second-order equations governing the transverse deflection and the rotation. The weak forms of these equations require Lagrange interpolation of the transverse deflection and rotation. Since the rotation function is like the (negative of) the derivative of the transverse deflection, the degree of the interpolation used for the rotation should be one less than that used for the transverse deflection. Such selective interpolation of the variables is called *consistent interpolation*. When the same interpolation functions are used to approximate the transverse deflection and the rotation, the resulting stiffness matrix is often too stiff to yield good solutions—especially when the number of elements used is small. This is due to the inconsistency of interpolation of the variables, and the phenomenon is known as *shear locking*. It is overcome by the use of reduced integration to evaluate the stiffness coefficients associated with transverse shear strains. The elements developed here are RIE, CIE-1, which has quadratic interpolation of the transverse deflection and linear interpolation of the rotation, and IIE.

The plane frame element based on the unified beam element (i.e., IIE) that contains the classical beam theory and Timoshenko beam theory have also been discussed. The frame element is a superposition of the beam and bar elements and has three degrees of freedom (axial displacement, transverse deflection, and rotation about an axis perpendicular to the plane of axial and transverse coordinates) per node. The general plane frame element is oriented at an angle from the horizontal position, and its equations are obtained by transforming the equations of the frame element in local coordinates.

## PROBLEMS

- 5.1 The natural vibration of a beam under applied axial compressive load  $N_0$  is governed by the differential equation

$$\frac{d^2}{dx^2} \left( EI \frac{d^2 w}{dx^2} \right) + N_0 \frac{d^2 w}{dx^2} = \rho A \omega^2 w$$

where  $\omega$  denotes nondimensional frequency of natural vibration,  $EI$  is the bending stiffness, and  $\rho A$  is the mass (mass density times cross-sectional area) of the beam. Develop (a) the weak form and (b) finite element model of the equation.

- 5.2 The differential equation governing axisymmetric bending of circular plates on elastic foundation is given by

$$-\frac{1}{r} \frac{d}{dr} \left[ \frac{d}{dr} (r M_{rr}) - M_{\theta\theta} \right] + kw = q(r)$$

where  $k$  is the modulus of the elastic foundation,  $q$  is the transverse distributed load, and

$$M_{rr} = -D \left( \frac{d^2 w}{dr^2} + \nu \frac{1}{r} \frac{dw}{dr} \right), \quad M_{\theta\theta} = -D \left( \nu \frac{d^2 w}{dr^2} + \frac{1}{r} \frac{dw}{dr} \right)$$

Develop (a) the weak form and identify the primary and secondary variables, and (b) the finite element model. Note that the shear force is defined by

$$Q_r = \frac{1}{r} \left[ \frac{d}{dr} (r M_{rr}) - M_{\theta\theta} \right]$$

- 5.3** The differential equations governing axisymmetric bending of circular plates according to the shear deformation plate theory are

$$-\frac{1}{r} \frac{d}{dr} (r Q_r) - q = 0 \quad (1)$$

$$-\frac{1}{r} \left[ \frac{d}{dr} (r M_{rr}) - M_{\theta\theta} \right] + Q_r = 0 \quad (2)$$

where

$$M_{rr} = D \left( \frac{d\Psi}{dr} + \nu \frac{\Psi}{r} \right), \quad M_{\theta\theta} = D \left( \nu \frac{d\Psi}{dr} + \frac{\Psi}{r} \right)$$

$$Q_r = K_s G H \left( \Psi + \frac{dw}{dr} \right)$$

where  $D = EH^3/[12(1-\nu^2)]$  and  $H$  is the plate thickness. Develop (a) the weak form of the equations over an element and (b) the finite element model of the equations.

- 5.4** Consider the fourth-order equation (5.2.1) and its weak form (5.2.4). Suppose that a two-node element is employed, with *three* primary variables at each node:  $w$ ,  $\theta$ , and  $\kappa$ , where  $\theta = dw/dx$  and  $\kappa = d^2w/dx^2$ . Show that the associated Hermite interpolation functions are given by

$$\phi_1 = 1 - 10 \frac{\bar{x}^3}{h^3} + 15 \frac{\bar{x}^4}{h^4} - 6 \frac{\bar{x}^5}{h^5}, \quad \phi_2 = \bar{x} \left( 1 - 6 \frac{\bar{x}^2}{h^2} + 8 \frac{\bar{x}^3}{h^3} - 3 \frac{\bar{x}^4}{h^4} \right)$$

$$\phi_3 = \frac{\bar{x}^2}{2} \left( 1 - 3 \frac{\bar{x}}{h} + 3 \frac{\bar{x}^2}{h^2} - \frac{\bar{x}^3}{h^3} \right), \quad \phi_4 = 10 \frac{\bar{x}^3}{h^3} - 15 \frac{\bar{x}^4}{h^4} + 6 \frac{\bar{x}^5}{h^5}$$

$$\phi_5 = -\bar{x} \left( 4 \frac{\bar{x}^2}{h^2} - 7 \frac{\bar{x}^3}{h^3} + 3 \frac{\bar{x}^4}{h^4} \right), \quad \phi_6 = \frac{\bar{x}^2}{2} \left( \frac{\bar{x}}{h} - 2 \frac{\bar{x}^2}{h^2} + \frac{\bar{x}^3}{h^3} \right)$$

where  $\bar{x}$  is the element coordinate with the origin at node 1.

- 5.5** Consider the weak form (5.2.4) of the EBE. Use a three-node element with two degrees of freedom ( $w$ ,  $\theta$ ), where  $\theta \equiv -dw/dx$ . Derive the Hermite interpolation functions for the element. Compute the element stiffness matrix and force vector. *Partial answer:*

$$\phi_1 = 1 - 23 \frac{\bar{x}^2}{h^2} + 66 \frac{\bar{x}^3}{h^3} - 68 \frac{\bar{x}^4}{h^4} + 24 \frac{\bar{x}^5}{h^5}$$

- 5.6–5.20** Use the minimum number of Euler–Bernoulli beam finite elements to analyze the beam problems shown in Figs. P5.6–P5.20. In particular, give:

- The assembled stiffness matrix and force vector.
- The specified global displacements and forces, and the equilibrium conditions.
- The condensed matrix equations for the primary unknowns (i.e., generalized forces) separately. Exploit symmetries, if any, in analyzing the problems. The positive convention used for the generalized displacements and forces is the same as that given in Fig. 5.2.2.

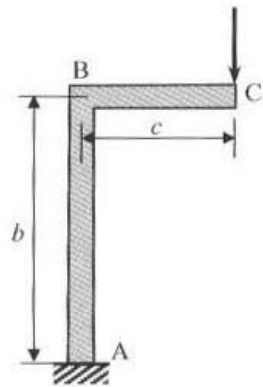


Figure P5.6

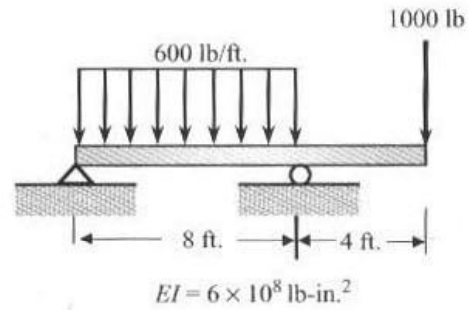


Figure P5.7

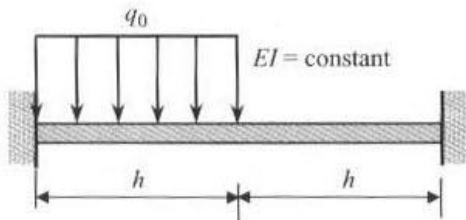


Figure P5.8

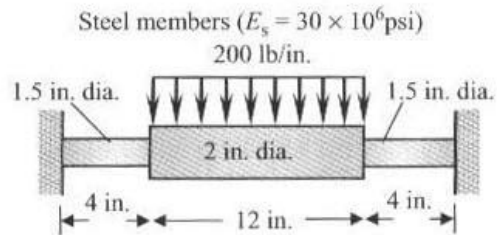


Figure P5.9

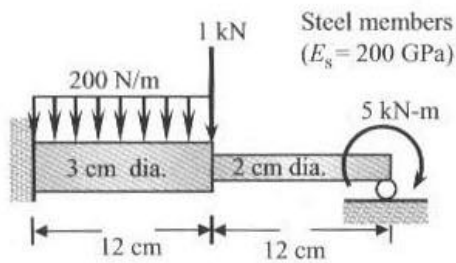


Figure P5.10

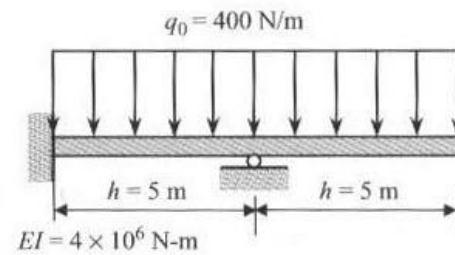


Figure P5.11

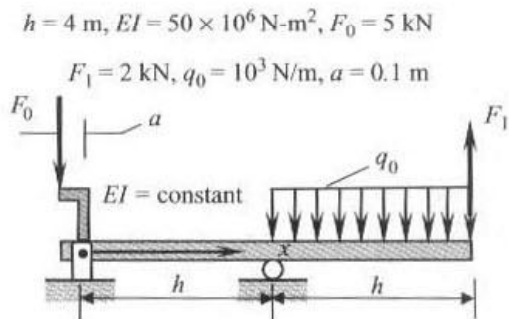


Figure P5.12

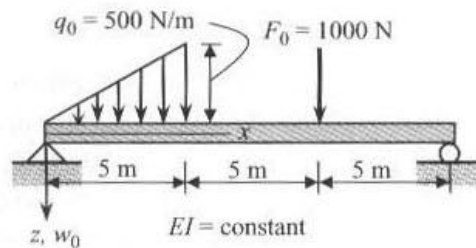


Figure P5.13

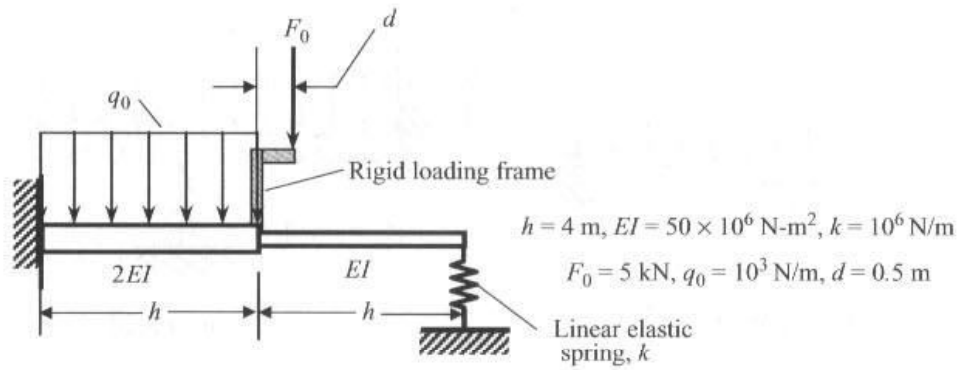


Figure P5.14

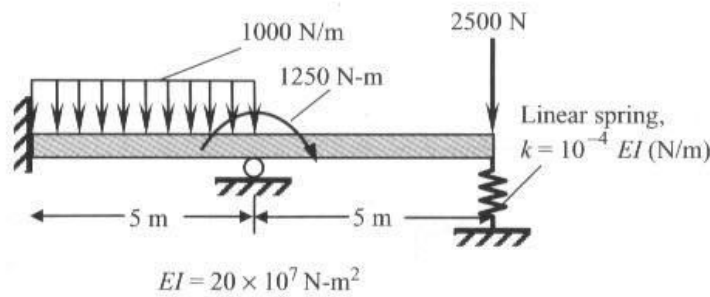


Figure P5.15

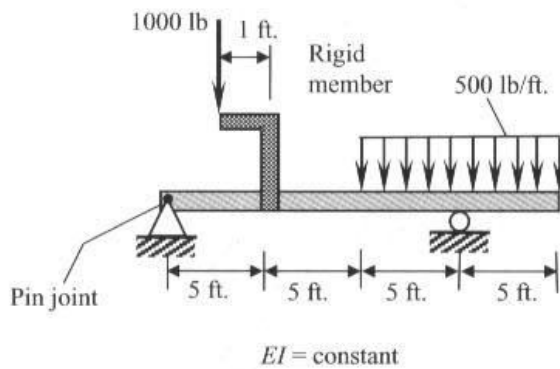


Figure P5.16

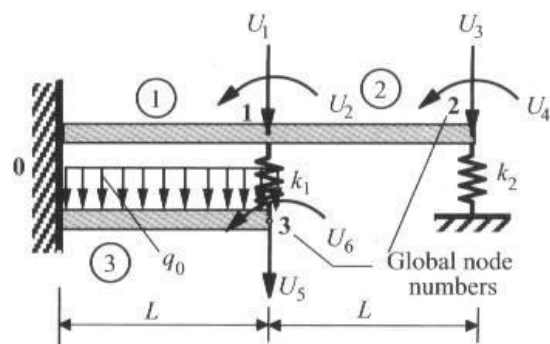


Figure P5.17

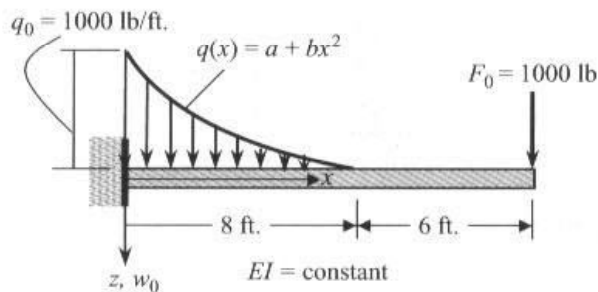


Figure P5.18

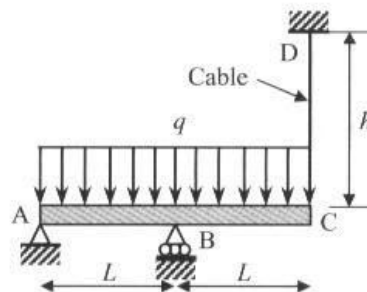


Figure P5.19

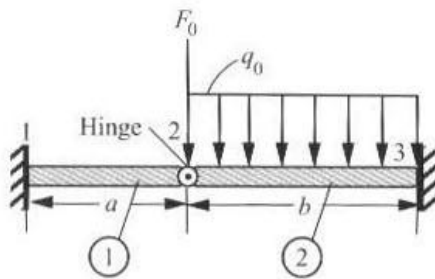


Figure P5.20

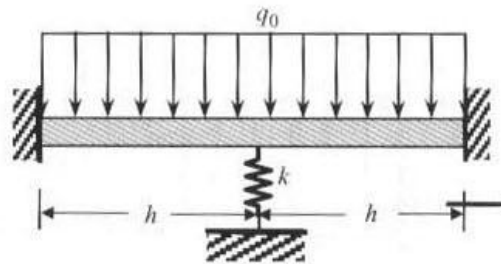


Figure P5.24

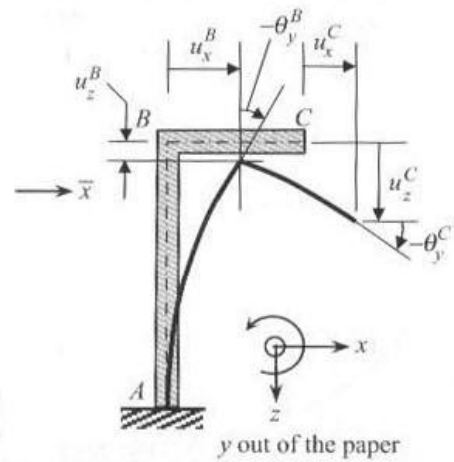
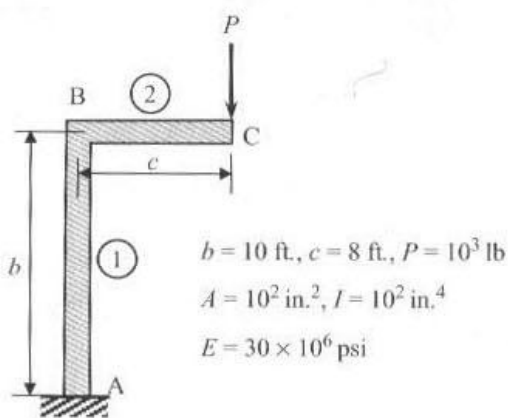
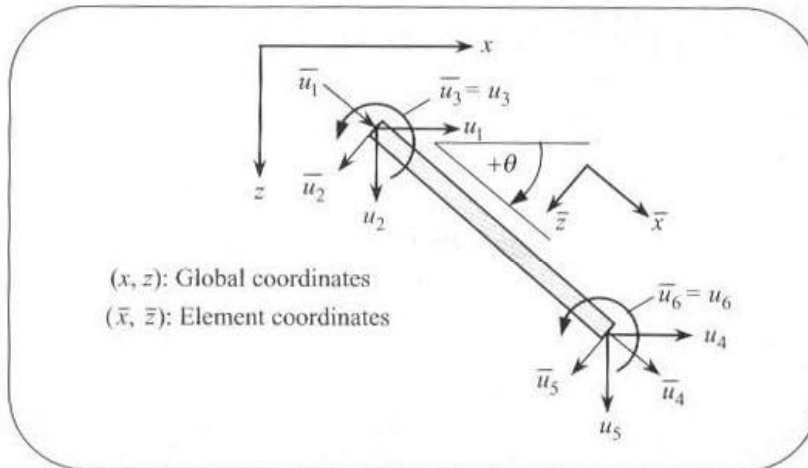
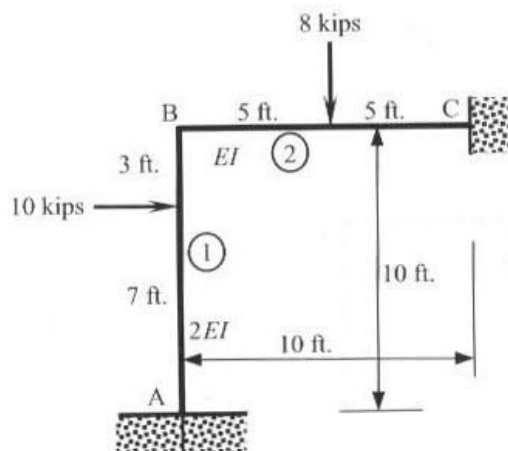


Figure P5.28

- 5.21 Analyze Problem 5.8 using the reduced-integration Timoshenko beam finite element (i.e., RIE). Use a value of  $\frac{5}{6}$  for the shear correction factor and  $\nu = 0.25$ .
- 5.22 Analyze Problem 5.8 using the consistent interpolation (quadratic  $w$  and linear  $\Psi$ ) Timoshenko beam element (i.e., CIE-1). Use a value of  $\frac{5}{6}$  for the shear correction factor and  $\nu = 0.25$ .
- 5.23 Analyze Problem 5.8 using the consistent interpolation (cubic  $w$  and quadratic  $\Psi$ ) Timoshenko beam element (i.e., CIE-2). Use a value of  $\frac{5}{6}$  for the shear correction factor and  $\nu = 0.25$ .
- 5.24 Analyze the problem in Fig. P5.24 using the consistent interpolation (quadratic  $w$  and linear  $\Psi$ ) Timoshenko beam element (i.e., CIE-1). Use a value of  $\frac{5}{6}$  for the shear correction factor and  $\nu = 0.25$ .
- 5.25 Analyze the problem in Fig. P5.24 using the consistent interpolation (cubic  $w$  and quadratic  $\Psi$ ) Timoshenko beam element (i.e., CIE-2). Use a value of  $\frac{5}{6}$  for the shear correction factor and  $\nu = 0.25$ .
- 5.26 Consider a thin isotropic circular plate of radius  $R_0$  and suppose that the plate is clamped at  $r = R_0$ . If two finite elements (see Problem 5.2) are used in the domain ( $0 \leq r \leq R_0$ ), give the boundary conditions on the primary and secondary variables of the mesh if the plate is subjected to (a) a uniformly distributed transverse load of intensity  $q_0$  and (b) point load  $Q_0$  at the center.
- 5.27 Repeat the circular plate problem of Problem 5.26 when a two-element mesh of Timoshenko elements is used.
- 5.28–5.35 For the frame problems shown in Figs. P5.28–P5.35, give (a) the transformed element matrices; (b) the assembled element matrices; and (c) the condensed matrix equations for the unknown generalized displacements and forces. Use the sign conventions shown in the figure below for global and element displacement (and force) degrees of freedom. The angle between the +ve  $x$ -axis and +ve  $\bar{x}$ -axis is measured in the clockwise sense.



$EI, EA$  are the same  
for the two members  
 $E = 30 \times 10^6 \text{ lb/in.}^2, \nu = 0.3$   
 $A = 100 \text{ in.}^2, I = 100 \text{ in.}^4$

Figure P5.29

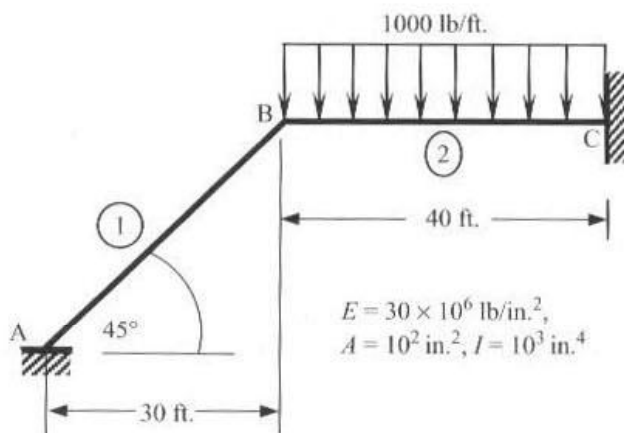


Figure P5.30

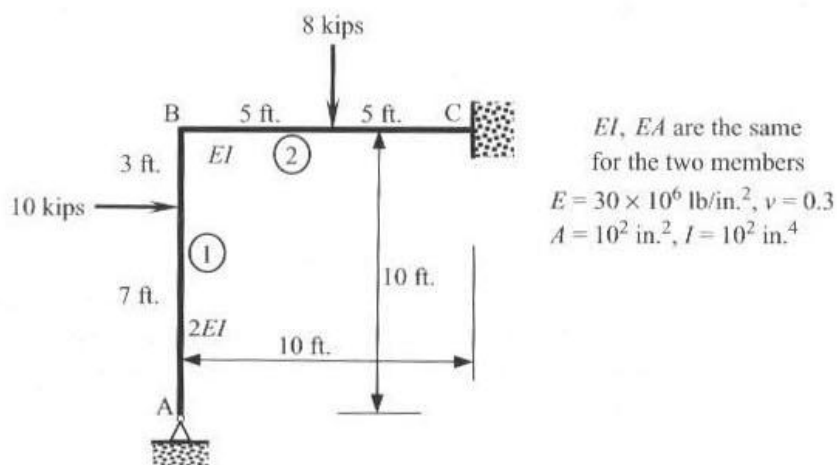


Figure P5.31

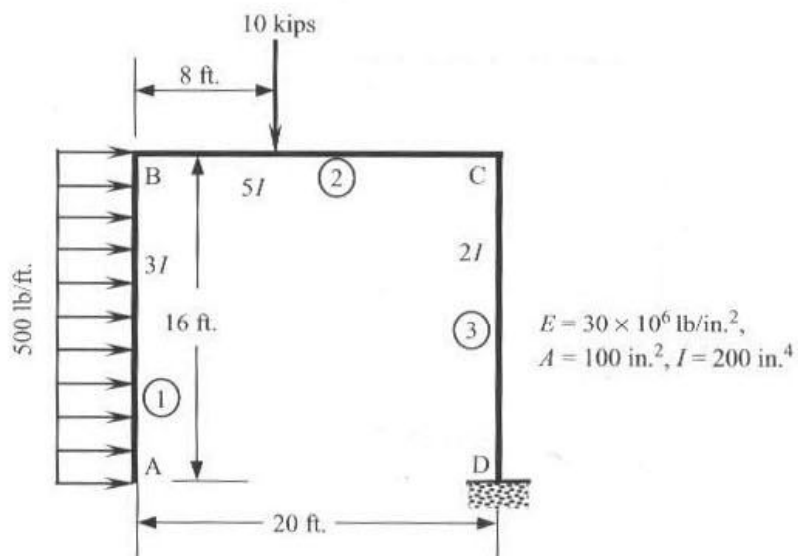


Figure P5.32

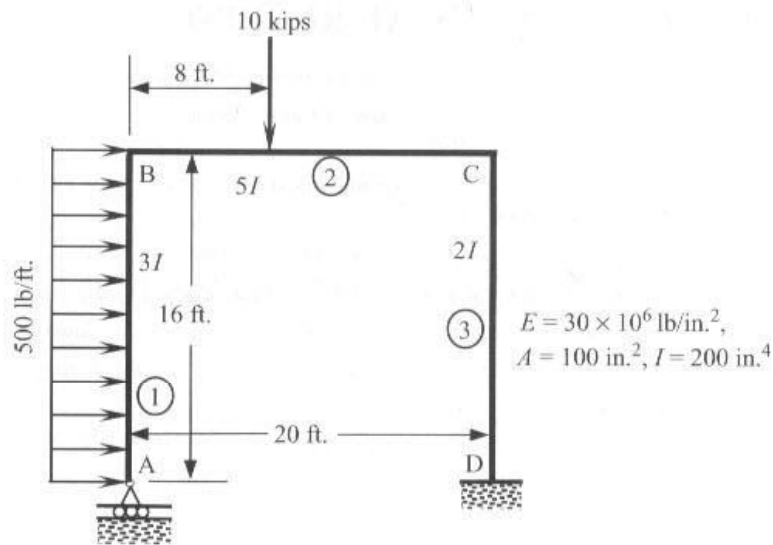


Figure P5.33

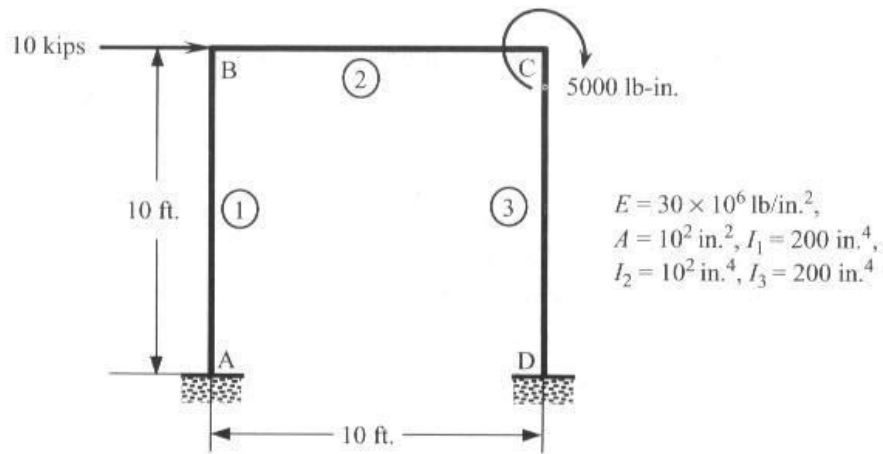


Figure P5.34

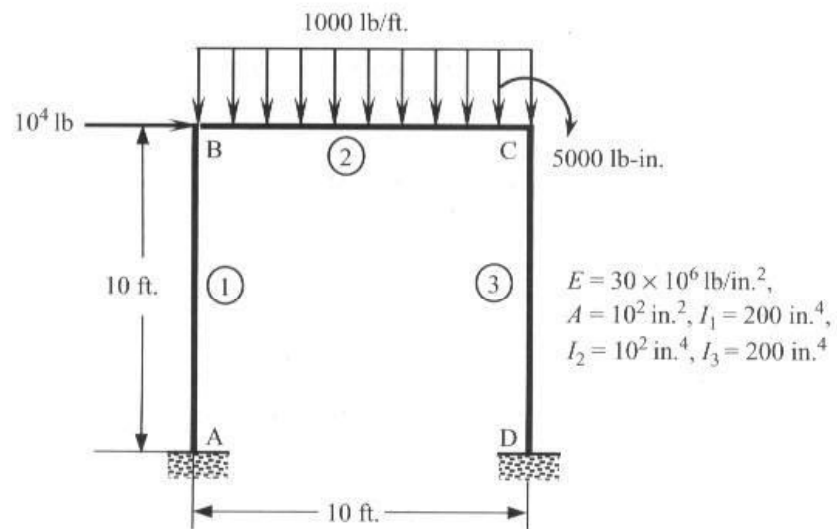


Figure P5.35

## REFERENCES FOR ADDITIONAL READING

1. Reddy, J. N., *Energy Principles and Variational Methods in Applied Mechanics*, John Wiley, New York, 2002.
2. Reddy, J. N., "On Locking-Free Shear Deformable Beam Finite Elements," *Computer Methods in Applied Mechanics and Engineering*, **149**, 113–132, 1997.
3. Reddy, J. N., "On the Derivation of the Superconvergent Timoshenko Beam Finite Element," *Int. J. Comput. Civil and Struct. Engng.*, **1**(2), 71–84, 2000.
4. Timoshenko, S. P. and Goodier, J. N., *Theory of Elasticity*, McGraw-Hill, New York, 1970.
5. Ugural, A. C. and Fenster, S. K., *Advanced Strength and Applied Elasticity*, Elsevier, New York, 1975.
6. Wang, C.-K. and Salmon, C. G., *Introductory Structural Analysis*, Prentice-Hall, Englewood Cliffs, NJ, 1984.
7. Wang, C. M., Reddy, J. N., and Lee, K. H., *Shear Deformable Beams and Plates. Relationships with Classical Solutions*, Elsevier, Oxford, UK, 2000.
8. Willems, N. and Lucas, Jr., W. M., *Structural Analysis for Engineers*, McGraw-Hill, New York, 1978.